2(mix)

THEORETICAL CHEMISTRY INSTITUTE

THE UNIVERSITY OF WISCONSIN

IMPULSIVE MODEL FOR REACTIVE COLLISIONS

Michael T. Marron and R. B. Bernstein

WIS-TCI-470

25 February 1972

MADISON, WISCONSIN

70P.

IMPULSIVE MODEL FOR REACTIVE COLLISIONS *

by

Michael T. Marron

Theoretical Chemistry Institute, University of Wisconsin, Madison, Wis. 53706

and Science Division, University of Wisconsin-Parkside,† Kenosha, Wis. 53140

and

R. B. Bernstein

Theoretical Chemistry Institute and Chemistry Department

University of Wisconsin, Madison, Wis. 53706

ABSTRACT

A simple classical mechanical model of the reactive scattering of a structureless atom A and a quasi-diatomic BC is developed which takes full advantage of energy, linear and angular momentum conservation relations but introduces a minimum of further assumptions. These are as follows: (1) the vibrational degree of freedom of the reactant (BC) and product (AB) molecules is suppressed, so the change in vibrational energy is simply a parameter; (2) straight-line trajectories are assumed outside of a reaction

- - - - - - - - - - - - - - -

* Supported by National Aeronautics and Space Administration Grant NGL 50-002-001, National Science Foundation Grants GB-16665 and GP-26014 (at Madison) and a grant from the Research Corporation (at Kenosha).

† Present address.

"shell" of radius R ; (3) within this zone, momentum transfer occurs impulsively (essentially instantaneously) following mass transfer; (4) the impulse $\underset{\sim}{I}$, which may be either positive or negative, is directed along the BC axis, which may, however, assume all orientations with respect to the incident relative velocity $\underset{\sim}{g}$. Assumption (3) is not as drastic as it appears since one may alternatively consider the reaction to have occurred on a potential surface such that the net force integrated over the entire "interaction region" yields the particular value of the impulse $\underset{\sim}{I}$. Differential and integral reaction cross sections are scaled according to R^2 (evaluated via molecular size considerations), but the model is not a member of the "hard-sphere" class. Potential surface information enters the model in two ways: (1) by the choice of sign of the impulse, positive corresponding to net exit-channel repulsion ("late-downhill" Polanyi-type), negative to a net approach-channel energy release ("early-downhill"); (2) by the weighting function for impulse directions, $\underset{\sim}{I}$ vs. $\underset{\sim}{g}$, i.e., the distribution function of (non-collinear) ABC configurations. The model yields differential and total cross sections and product rotational energy distributions for a given collision exoergicity Q , or for any known distribution over Q . Numerical results are presented for several prototype reactions whose dynamics have been well-studied in several molecular beam scattering laboratories. Many of the main experimental features are readily accounted for by the model without adjustment of parameters. However, it is difficult to reproduce the often-found "uncoupling" of the product angular and recoil energy distributions.

I. INTRODUCTION

Molecular beam, chemiluminescence, and chemical laser experiments are rapidly expanding our experimental knowledge of reaction dynamics.[1] Our theoretical understanding is also increasing, but it lags somewhat behind experiment. Although quantum, semiclassical and classical approaches are all being intensively pursued,[2] up to the present time classical trajectory studies[3] have probably contributed most to our understanding of the relationships between potential surface and the observable dynamics. The present paper considers a further-simplified, classical treatment of (model for) the 3-body exchange reaction.

In light of advances at a more fundamental level one may question the role of such simplified models in the field of reaction dynamics. First, it is noted that when approximations are made to a more rigorous theory, in addition to facilitating calculation, one often tests the physical basis underlying the approximations and thus gains a deeper physical insight into the collision process. Second, one can hope to correlate trends for series of related reactions. Third, one can attempt to identify reaction features which can be attributed primarily to the existence of kinematic constraints (such as the conservation relations) so that those features most sensitive to potential surface characteristics may be isolated.

In this paper a new classical model for reactive collisions of the type $A + BC \rightarrow AB + C$ is developed, which is more general than the familiar hard-sphere models but which retains their attractive feature whereby all dynamical quantities follow from the equations of conservation of energy and momenta. The central theoretical construct of the model is

the impulse of a collision, defined as the force between two bodies integrated over the entire trajectory. This impulse $\underset{\sim}{I}$ (units of momentum) may be viewed as the net momentum transfer in the course of the reaction. In some average sense, the impulse has extracted all the necessary information from the interaction potential. Because (or perhaps in spite) of this simplistic characterization of the interparticle interactions, the model applies both to reactions which occur on a single potential surface and to reactions involving potential surface crossings.

Before proceeding, it is of interest to list the existing simple classical models. Excluded are statistical models,[4] and those which deal exclusively with ion-molecule reactions.[5]

Hirschfelder and Wigner[6] and Hulbert and Hirschfelder[7] performed quantal calculations of transmission coefficients for particles under the influence of idealized potential surfaces, which were followed by classical mechanical calculations for these same surfaces.[8] The harpoon (electron-jump) model was developed by Magee[9] to account for the large rates of flame reactions involving alkali atoms. One of the first fully classical models for reaction dynamics was the so-called billiard-ball (BB) model of Libby,[10] applied to hot atom reactions to obtain the probability of reaction as a function of translational energy. BB models continued to be used[11] until Cross and Wolfgang[12] showed the inaccuracy of the BB model in predicting the energy-weighted total cross section (the so-called reaction integral). There have been criticisms[13,14] of this conclusion and alternative BB models have been proposed.[14] Most recently Baer and Amiel[15] have extended the simple BB model to include idealized potential surfaces and have obtained improved results.

From the viewpoint of the classical kineticist the most important model is that of Fowler and Guggenheim,[16] i.e., the familiar hard-sphere model in which reaction occurs if the component of the relative velocity along the line-of-centers at collision exceeds a threshold value. Present[17] placed this model on firmer theoretical grounds when he recast it in terms of the potential energy surface and its relation to activation energy. Extensions of this model have been made by Levine.[18] Marron[19] has discussed this model and a similar one which is based on consideration of the energy and momentum of the reactants and the products. Other modifications of the simple hard-sphere model for reactions include those by Herschbach,[20] Beuhler and Bernstein,[21] and Grice.[22]

A different type of reaction model is the spectator stripping (SS) one which was borrowed from the theory of direct nuclear reactions.[23] This model was first applied to ion-molecule reactions and then to the alkali atom-halogen reactions by Minturn et al.[24] Herschbach[20] has suggested a modification of the SS model which adds the internal momentum of BC to the final AB momentum to produce a broadening of the angular distribution. Herman et al.[25] have also suggested a modified form of the SS model, in which polarization forces are considered explicitly. Chang and Light[26] have extended it further by making additional dynamical assumptions. Two other models,[27,28] very similar in nature, are directed primarily to the problem of estimating energy partitioning between translational release and vibrational excitation of products.

Another class of models, which leads to the present model, might be termed advanced hard-sphere models. Suplinskas[29a] has described a hard-

sphere model for reactions A + BC, where each atom is represented by a sphere, and extended the model[29b] by including an attractive long-range force similar to that of Ref. 25. A final case is the DIPR model of Kuntz et al.[30] which has provided part of the inspiration for this work. The DIPR model was developed to fit the results of extensive classical trajectory calculations for reactions forming an ionic bond, and has been fairly successful when applied to ion-molecule reactions.[30c,31]

The DIPR model allows calculation of the scattering angle by considering the C atom which is deflected from its original path by a force along the original BC-axis direction. It may be viewed alternatively as a hard-sphere model in which A approaches BC with no interaction until a fixed reaction distance is reached, then B changes partners and momentum transfer of a specified magnitude occurs instantaneously in the BC-bond-axis direction. The rather drastic assumption of instantaneous momentum transfer may be softened by adopting a pseudo-hard-sphere view which defines the reaction radius as the point of mass transfer and defines the impulse (net momentum change) as occuring in some direction (e.g., the original BC-axis direction) to be averaged over, and operating initially on the system A + BC and finally on AB + C . This is tantamount to enclosing the interaction region in a "black box" and spcifying the net momentum transfer. By observing how A and BC enter the box one can calculate the AB and C exit angles and recoil energy. If one assumes a particular separation at which mass transfer occurs, the rotational energy of AB may also be calculated. By varying the relative A—BC orientation and impact parameter, the angular and energy distribu-

tions may be computed.[30] While Kuntz et al. have not described the DIPR model in these same terms, the equivalence can be shown.[32] A distinct advantage of the DIPR model over many others is that it is possible to derive analytical expressions for the energy and angular distributions.[30d,32] A second advantage of the DIPR model is that the free parameters ("loose screws") such as the magnitude of the impulse, orientation weighting, etc. can be related roughly to potential parameters.[30,33]

The present model, though closely related to the DIPR model, differs significantly in one way: instead of assuming the magnitude of the impulse and calculating the final energy of the products, one specifies the latter and calculates the coresponding value of the impulse and thus the angular (and rotational state) distribution of the products. This is of some practical value in connection with modern molecular beam experiments employing the velocity-selection and -analysis technique.[34] The hope is that those features of the scattering which are due primarily to kinematic or conservation constraints can be isolated from those due to potential surface characteristics. When both the initial and final translational (c.m.) energies are specified the energy and momentum transfers are those required by the conservation equations. Calculations with the present model indicate that these constraints, together with a small amount of information about the potential surface, suffice to explain the main features of the angular distribution of products.

II. CONSERVATION EQUATIONS AND MODELS

On the one hand a simple, easily-soluble model is desirable yet it must be sufficiently flexible to permit a description of a variety of systems. Light's definition[26] of a model is, "two trajectories connected by an assumption." Here the "trajectory" is that portion of a collision before (after) the reactants (products) feel significant mutual interaction. The initial and final trajectories are then directly related by the conservation equations:

$$(A+B)\,\underset{\sim}{w}_{AB} + C\,\underset{\sim}{w}_{C} = A\,\underset{\sim}{w}_{A} + (B+C)\,\underset{\sim}{w}_{BC} \qquad (1)$$

$$\underset{\sim}{L}' + \underset{\sim}{j}' = \underset{\sim}{L} + \underset{\sim}{j} \qquad (2)$$

$$E'_{tr} + E'_{rot} + E'_{vib} = E_{tr} + E_{rot} + E_{vib} + \Delta D_o \,. \qquad (3)$$

Equation (1) expresses conservation of linear momentum; A, B, and C represent the masses of the particles A, B and C and $\underset{\sim}{w}_i$ is the velocity of the i th particle relative to the center of mass (c.m.). Equation (2) represents conservation of angular momentum; $\underset{\sim}{L}$ is orbital angular momentum, and $\underset{\sim}{j}$ is rotational angular momentum; primes denote final quantities. Equation (3) expresses conservation of energy; ΔD_o is the appropriate difference in zero-point dissociation energies bond (positive for exoergic reactions). In the present model there is no vibrational degree of freedom, so $E_{vib}-E'_{vib}$ is simply a parameter. For purposes which will become clear, it is preferable to write the conservation equations differently, in terms of the impulse $\underset{\sim}{I}$ and the relative

velocity $\underset{\sim}{g} = \underset{\sim}{w}_A - \underset{\sim}{w}_{BC}$, $\underset{\sim}{g}' = \underset{\sim}{w}_{AB} - \underset{\sim}{w}_C$. Thus
$E_{tr} = \frac{1}{2}\mu g^2 = \frac{1}{2}A(B + C)g^2/(A+B+C)$. Equation (1) becomes

$$A\,\underset{\sim}{w}_A + B\,\underset{\sim}{w}_{BC} - (A+B)\,\underset{\sim}{w}_{AB} = -C\,\underset{\sim}{w}_{BC} + C\,\underset{\sim}{w}_C \,. \qquad (4)$$

Equating both sides to $\underset{\sim}{I}$ gives:

$$\frac{AC}{(A+B+C)}\,\underset{\sim}{g} - \frac{(A+B)C}{(A+B+C)}\,\underset{\sim}{g}' = \underset{\sim}{I}\,, \qquad (5)$$

or, alternatively

$$f\,\underset{\sim}{p} = \underset{\sim}{I} + \underset{\sim}{p}' \qquad (6)$$

where $\underset{\sim}{p} = \mu\underset{\sim}{g}$ the initial relative momentum, $\underset{\sim}{p}' = \mu'\underset{\sim}{g}'$ the final momentum and $f \equiv C/(B + C)$. The partitioning of Eq. (1) to form Eq. (4) is somewhat arbitrary and could also be done:

$$A\,\underset{\sim}{w}_A - (A+B)\,\underset{\sim}{w}_{AB} = C\,\underset{\sim}{w}_C - (B+C)\,\underset{\sim}{w}_{BC} \qquad (4')$$

which also yields Eq. (6) with $f = 1$. The difference is one of a scale factor. The first form has been chosen, to agree with the DIPR model.[30] Eq. (5) may also be written

$$C\,\underset{\sim}{w}_C = C\,\underset{\sim}{w}_{BC} + \underset{\sim}{I}\,. \qquad (5')$$

This implies that the particle C initially travelling with the velocity of BC , i.e., $\underset{\sim}{w}_{BC}$ is deflected from its path by the impulse $\underset{\sim}{I}$ to velocity $\underset{\sim}{w}_C$. The scattering angle, say χ , is thus defined as the angle between $\underset{\sim}{p}$ and $\underset{\sim}{p}'$. The physical distinction between (4) and (4') is that the impulse occurs <u>after</u> mass transfer for (4) but before mass transfer for (4').

The conservation equations are not, in themselves, sufficient to determine the collision dynamics, i.e., given a set of initial conditions the final trajectory cannot be determined. This is due to the fact that there are 7 equations, (two vector, Eqs. (2), (6) and one scalar, Eq. (3)) and 10 unknowns: $\underset{\sim}{L}'$, $\underset{\sim}{j}'$, $\underset{\sim}{g}'$, and $E_{vib}-E'_{vib}$. The model is a set of assumptions which implies values for any three of these ten unknowns.

III. DERIVATION OF THE MODEL

Initial experimentation with various hard-sphere models revealed that the requirement of momentum transfer along the line-of-centers produces only "backscattering" of the reaction products.[35] Figure 1a illustrates the vector relationship expressed in Eq. (6) for conservation of momentum; it can be seen that if the impulse lies in the same (forward) direction as the initial relative velocity, as it almost always does for line-of-centers momentum transfer, the final relative velocity will be directed backward. In order to obtain a model that will produce forward and/or backward scattering the impulse must be permitted to assume all angles with respect to the incoming $\underset{\sim}{p}$. One method of achieving this goal is to discard the line-of-centers assumption for $\underset{\sim}{I}$ and assume that $\underset{\sim}{I}$ must be directed along the B-C bond axis. Since the orientation of the target molecule BC is not restricted, $\underset{\sim}{I}$ can then take on all directions. The concept of a hard spheres is used only to determine the "reaction radius" R (the distance between A and the c.m. of BC) which is the point on the initial trajectory at which mass transfer occurs. It is assumed that momentum transfer occurs impulsively, though not as it would for hard spheres. The assumption of instantaneous momentum transfer serves to simplify the solution of the equations of motion in that the conservation equations then contain all the system dynamics. If one prefers, the reaction may be viewed as having occured on some potential surface with a net force, integrated over the entire interaction region, in the direction of $\underset{\sim}{I}$ and having a magnitude $|\underset{\sim}{I}|$. These two viewpoints are formally equivalent.[36]

The coordinate system is shown in Fig. 1b. The direction of the z-axis is that of the initial relative velocity $\underset{\sim}{g}$; the orientation of the target upon collision is given by the angles θ (the rotation of C about the BC center-of-mass c.m. in the XZ plane) and ϕ , the azimuthal rotation about the z-axis. The scattering angle χ is defined by

$$\cos\chi = \underset{\sim}{p}\cdot\underset{\sim}{p}'/(pp') . \tag{7}$$

Squaring Eq. (6) gives

$$I^2 = (fp)^2 + (p')^2 - 2fpp'\cos\chi . \tag{8}$$

Defining the dimensionless parameter

$$\alpha \equiv p'/fp , \tag{9}$$

Eq. (8) is rewritten

$$I/fp = (1 - 2\alpha\cos\chi + \alpha^2)^{1/2} . \tag{10}$$

The z-component of Eq. (6) is

$$\alpha\cos\chi + (I/fp)\cos\theta = 1 . \tag{11}$$

Then θ can be expressed in terms of χ :

$$\cos\theta = (1 - \alpha\cos\chi)/(1 - 2\alpha\cos\chi + \alpha^2)^{1/2} . \tag{12}$$

Eq. (11) may be substituted into (10) to yield the inverse relationship for $\chi(\theta)$:

$$\cos\chi = \left(\frac{1}{\alpha}\right)\left[\sin^2\theta \pm \cos\theta\,(\alpha^2 - \sin^2\theta)^{1/2}\right] \tag{12'}$$

where the negative square root is implied if $\alpha \geq 1$; both roots are taken if $\alpha < 1$ and $0 \leq \sin\theta \leq \alpha$. Note that the scattering angle χ is independent of the azimuthal angle ϕ of the target. It can also be shown that the azimuthal angle of the trajectory, say ψ , is identical to ϕ . Eq. (12') indicates that the scattering angle χ is independent of impact parameter, b (the perpendicular distance between A and the z-axis at collision). The final rotational energy, E'_{rot}, however, depends on both b and ψ.

A. Potential Surface Information

Before going on to derive expressions for product angular and rotational energy distributions it is of interest to note that qualitative potential surface information may be introduced at this point by two means. First, the sign of the impulse can be chosen as positive or negative. Following Polanyi,[37] this might correspond to whether the potential is of the "early-downhill" or "late-downhill" type, i.e., whether energy is released primarily in the approach channel, A + BC, or the exit channel, AB + C. Since in the model the impulse occurs after mass transfer (i.e., Eq. (4) instead of (4')),a positive impulse corresponds to a net exit-channel repulsion while a negative impulse indicates a net approach-channel energy release.[38] These concepts are discussed in more detail in Ref. 30.

A second means of introducing potential information is to weight different impulse directions, i.e., target orientations, differently. For example it is known[21] that in the reaction $M + CH_3I \rightarrow MI + CH_3$, the alkali atom attacks the iodine end of CH_3I preferentially. On the other hand,

for an alkali attack on HBr (where the Br atom is much larger than the H atom) much less orientation dependence is expected. The simplest possible weighting function is one involving only the angle θ (see Fig. 1b). A convenient functional form is

$$R_\theta = A\,(1 + \cos\theta)^n \tag{13}$$

where A is a normalization constant. The plus or minus sign is chosen according to whether the B or the C end of the molecule is reactive. The power n determines how rapidly R_θ drops to zero. Note also that by virtue of Eq. (11) and because of the symmetry in the form of R_θ, changing the sign in front of $\cos\theta$ is equivalent to changing the sign of the impulse $\vec{I}$. A sign change may thus be considered <u>either</u> a change in which atom of BC is most reactive <u>or</u> a change in the sense of the impulse $\vec{I}$. (A change in both leaves the sign in (13) unchanged.) This equivalence exists only because of the symmetry inherent in R_θ due to the fact that $\vec{I}$ is assumed to be directed along the BC axis.

The weighting function (13) is not simply related to the A-B-C configuration angle, say ζ, i.e., the angle between $\vec{R}$ and the BC axis (see Fig. 1b). Another choice for the weighting function is

$$T_\theta = A'(1 \pm \cos\zeta)^{n_{BC}} \tag{14}$$

where A' is a constant and $\cos\zeta$ is given by

$$\cos\zeta = \sin\gamma \sin\theta\cos\phi + \cos\theta\cos\gamma. \tag{15}$$

The angle ζ depends on both the orientation (θ,ϕ) of BC at collision and the impact parameter $b = R \sin\gamma$, where γ is the angle between $\underset{\sim}{R}$ and $\underset{\sim}{g}$ (see Fig. 1b). Averaging over impact parameter must now be carried out explicitly. For the case $n = 1$, averaging over ϕ and b yields:

$$\langle T_\theta \rangle \propto \int_0^{\pi/2} d\gamma \int_0^{2\pi} d\phi \, \sin\gamma \cos\gamma \cos\zeta \propto 1 \pm \tfrac{2}{3}\cos\theta . \tag{16}$$

(Similar equations can easily be found for $n \neq 1$.) Comparing R_θ and $\langle T_\theta \rangle$ we see that the effect of weighting by $\cos\zeta$ instead of $\cos\theta$ is to give a higher relative weight to target orientations in the region of θ near $\pi/2$. This is reasonable because both R_θ and T_θ give the largest weighting to collinear configuration but R_θ fails to take account of the fact that collinear configurations exist for all θ.

In both of the two weighting schemes above a step function $\mathcal{H}(R-b)$ has been assumed for the impact parameter dependence ($\mathcal{H}$ is the Heaviside function). A more realistic form[39] for $P_b(b)$ has a maximum at $b = 0$ and decreases monotonically to zero at some b, say R. This form reflects the fact that collisions at large b have only a small radial velocity component; even a collinear collision at large b is less likely to result in reaction than a collinear collision at $b = 0$. As an illustrative calculation the functional form $P_b \propto \cos^2\gamma$ has been used. The major effect of including this P_b is to counteract the change noted in going from R_θ to $\langle T_\theta \rangle$, that is target orientations with θ near 0 and π are reemphasized over orientations near $\theta = \pi/2$. The weighting functions R_θ, $\langle T_\theta \rangle$ and $\langle T_\theta \cdot P_b \rangle$ are plotted in Fig. 2

for the chosen $P_b \propto \cos^2\gamma$ and $n = 1$. The brackets indicate averaging over b and ϕ. Because of the similarities between R_θ and the most "realistic" weighting function $\langle T_\theta \cdot P_b \rangle$ and because there is no simple *a priori* way to determine either T_θ or P_b, the convenient, simplest form, R_θ, is employed for the remainder of the discussion.

B. Differential Reaction Cross Sections

The formula for the differential reaction cross section may be derived from a formal definition of the cross section[40] in terms of the model variables

$$d^6\sigma_R = d^2S(\eta)\, d^2G(\mathcal{T})\, d^2H(\omega) \tag{17}$$

where η refers to the pair of variables b,β (β is the azimuthal angle of R), $\mathcal{T}$ refers to the orientation θ,ϕ (see Fig. 1) and ω to the scattering angles χ,ψ. The differential "area" on the left is proportional to the product of probabilities that for collisions in the range η to $\eta + d\eta$ and for target (BC) orientations in $\mathcal{T}$ to $\mathcal{T} + d\mathcal{T}$, the AB product will be scattered into a solid angle in the range ω to $\omega + d\omega$. The details of the derivation may be found in Appendix I. For the present model, Eq. (17) reduces to

$$\frac{d^2\sigma_R}{d^2\omega} = \frac{\sigma}{4\pi} P_\theta(\theta_\chi) \frac{\alpha^2 |(\alpha - \cos\chi)|}{(1 - 2\alpha\cos\chi + \alpha^2)^{3/2}} \tag{18}$$

where $\sigma \equiv \pi R^2$ and P_θ is the desired configuration weighting function. The argument is subscripted to indicate the one-to-one relationship between χ and θ. Eq. (18) will be discussed further in Sec. IV and applied to a number of systems of experimental interest in Sec. V.1.

C. Total Reaction Cross Section

The reaction cross section σ_R is found by integrating Eq. (18) over all solid angles. Because of the absolute value in the numerator of Eq. (18) two cases must be distinguished: $\alpha > 1$, $\alpha \leq 1$. Assuming that P_b is the step function $\mathcal{H}$ (R-b) and $P_\theta = 1$, direct integration yields

$$\sigma_R = \sigma \qquad (\alpha > 1)$$
$$= \sigma\left[1 - (1-\alpha^2)^{1/2}\right] \qquad (\alpha \leq 1). \tag{19}$$

If a weighting function other than $\mathcal{H}$(R-b) is used for impact parameter and/or if any weighting function is introduced for orientation, the total reaction cross section is necessarily diminished. The actual decrease depends on the explicit form chosen for P_θ and/or P_b. Equation (19) is in agreement with the previous work[19] on simple hard spheres where it was found that the total reaction cross section has an energy dependence only when $\alpha \leq 1$. Note that the present α differs by a factor of $C/(B + C)$ from that in Ref. 19.

D. Product Rotational Energy

The rotational energy, E'_{rot}, of the products may be determined via Eq. (2); details are given in Appendix II. It is found that E'_{rot} depends

$$E'_{rot}(\underset{\sim}{g}, \underset{\sim}{g}', b, \theta, \phi), \tag{20}$$

upon the system parameters R, μ and μ', $\underset{\sim}{g}$ and $\underset{\sim}{g}'$ (which are given, the direction $\underset{\sim}{g}'$ defined by the scattering angle), and b, θ, ϕ defining the reaction configuration. One must average over b, ϕ and ψ (including any desired weighting function) to determine the contribution from all configurations, to yield the quantity $\langle E'_{rot} \rangle$. The brackets $\langle\ \rangle$ denote such an average over b, ϕ, and ψ. This calculation has been carried out in Appendix II. Then $\langle E'_{rot} \rangle$ depends only on χ and on the ratio g'/g in addition to the system parameters. The result of this averaging can be expressed by means of the dimensionless quantity δ_{rot}, defined

$$\delta_{rot} \equiv \frac{4\pi}{(\mu g R)^2} \left\langle j'^2 - j^2 \right\rangle$$

$$= 1 + 2f(g'/g)\cos\chi + (g'/g)^2 \left[f^2 + (f^2 \sin^2\chi)/2 \right.$$

$$\left. + \frac{8}{3}\left(\frac{r_{ac}}{R}\right)\frac{BC^2(A+B+C)}{A(B+C)^3}\sin\chi\sin(\chi-\theta) + 2\left(\frac{r_{ac}}{R}\right)^2 \frac{B^2C^2(A+B+C)^2}{A^2(B+C)^4}\sin^2(\chi-\theta) \right], \quad (21)$$

where $f \equiv C(B+C)^{-1}$. Equation (21) is applied to several systems in Sec. V.2.

IV. BEHAVIOR OF DIFFERENTIAL REACTION CROSS SECTION

The model predictions depend on the choice of values for R, for $P(\alpha)$ (or equivalently $P(E')$), i.e., the distribution of α; the sign of the impulse; and the configuration weighting function. In this section the behavior of the differential cross section is examined as a function of each of these quantities.

The reaction distance R enters the differential cross section for the reaction first as a scale factor, i.e., scaling the differential and total cross section according to R^2, and secondly as it affects the final rotational energy distribution (cf. Appendix II). Insofar as angular distributions are concerned the effect of R may be ignored.

The value of α and its probability density depend upon the final translational energy and its distribution, $P(E')$. In the present model these quantities are either to be guessed or taken from experiment. It will be seen that the angular distribution calculated from the model is not extremely sensitive to the choice of $P(E')$. Unfortunately, this implies that the inverse use of the model to determine $P(E')$ from the angular distribution is unlikely to yield useful results.

The final two quantities, the sign of the impulse and the weighting function, serve to characterize the potential surface for the reaction. Here one must exercise chemical intuition and allow the experiments to serve as confirmation.

In Fig. 3 angular distributions $d^2\sigma_R(\chi)/d^2\omega$ are plotted for various choices of alpha and the weighting function R_θ given in Eq. (13). As mentioned before, because of the inherent symmetry of R_θ a change of

sign is equivalent to either interchanging the "reactive" end of BC or changing the sign of the impulse. If the limit of Eq. (18) is taken as $\alpha \to \infty$ we obtain

$$\frac{d^2\sigma_R}{d^2\omega} = \frac{\sigma}{4\pi} R_\theta \qquad (\alpha \to \infty). \tag{22}$$

Thus, for large α and no weighting ($n = 0$) the angular distribution is nearly isotropic. When weighting is included, i.e., $P_\theta \neq 1$, the angular distribution reflects entirely the weighting function. On the basis of this model, we expect that for experimental situations characterized by large α, the angular distribution of the products will be very sensitive to potential surface features.[41] This condition obtains in either of two situations: first, when the collisional exothermicity $Q = E' - E$ is very large (i.e., the AB molecules are produced in low-lying internal states and ΔD_o is large), and second when the mass B is much larger than the mass of A or C. This last result is easily seen by considering the limit of α for $\frac{B}{A}, \frac{B}{C} >> 1$. Here

$$\alpha = \left[\frac{(B+C)(A+B)}{AC}\,\frac{E'}{E}\right]^{1/2} \to \frac{B}{\sqrt{AC}}\left(\frac{E'}{E}\right)^{1/2}. \tag{23}$$

As α approaches 1 from above, the unweighted ($n = 0$) distribution increases rapidly in the forward direction. When a weighting function is included, the angular distribution can be shifted either in the forward or backward direction or even (e.g., in the case $\alpha = 2$ and $n = +1$) to produce side-scattering. Forward scattering obtains when $\alpha \to 1$ since a large fraction of target configurations yield products in the hemisphere; in fact, all configurations with $\theta \geq 90°$ yield products

within a ca. 1° forward cone. Inclusion of a weighting function serves either to emphasize the minority configurations which produce proportionally more products in the backward direction or vice versa. If the magnitude of the impulse is computed for a value of α just slightly greater than 1.0, say $\alpha = 1.001$, it is found to vary between 2.0 and 0.0 (in units of the initial momentum μg) with $I \approx 0.01$ for those configurations which yield foward scattering.

It is instructive to compare the $\alpha = 1$ case with the predictions of the spectator stripping (SS) model.[20,24] The essence of the SS model is that atom C is a spectator to the reaction and will continue with velocity and direction unchanged after loss of B . Thus $\underset{\sim}{w}_{BC} = \underset{\sim}{w}_{C}$, which implies together with Eqs. (4) and (5) that $\underset{\sim}{I} = 0$ or that

$$f \underset{\sim}{p} = \underset{\sim}{p}' \quad . \tag{24}$$

Using Eq. (7) the scattering angle may be computed, which yields the well-known result that the products are always scattered at $\chi = 0$. The SS limit cannot be obtained directly from Eq. (18) because we can only include one of the three SS constraints exhibited in Eq. (24), that is $\alpha = 1$. The limit ($\alpha \to 1$) applied to Eq. (18) yields an infinite differential cross section for $\chi \to 0°$, reminiscent of the classical divergence in the differential elastic scattering cross section at 0° for all but rigid spheres. The SS limit can of course be derived directly from Eq. (6) where all three constraints may be included.[42]

For values of $\alpha < 1$, Eq. (18) has a zero at $\chi = \cos^{-1}\alpha$. The physical reason for the zero is that not all possible reaction configurations can produce a reaction. Fig. 4 is a plot, for $\alpha = 0.8$, of the configura-

tion angle θ versus the scattering angle χ . For configurations $\theta > 53°$, reaction cannot occur satisfying the conservation relations.[43] This condition is not unique to this model but is found in other models in which energy partitioning is specified. When the angular distribution is averaged over any reasonable final energy distribution the zero disappears and predominantly forward scattering obtains. Inclusions of the weighting function, R_θ , will modify the angular distribution; but forward scattering persists. As α tends to zero the differential cross section and the total cross section (cf. Eq. (19)) also tend to zero. The situation characterized by small α arises only for instances of negative Q .

It should be noted that the joint angular-recoil energy distribution is a coupled function of χ and E' (via α) . For "rebound" scattering (i.e., positive impulse) the angular distribution shifts from sharply backward to broad, as alpha decreases. When the impulse is negative, the angular distribution is found to be broad, slightly favoring the forward direction for large α , and as α is decreased the scattering is progressively concentrated in the forward hemisphere.

V. APPLICATION OF MODEL

A. Angular Distributions

In this section the differential reactive cross sections are calculated for several systems which have been studied experimentally. It will be seen that for reasonable choices of the weighting function, good agreement can be obtained between the model and experimental results. Further, the model can explain the observed trends of the reactive scattering for members of a homologous series. The results described show thereby that many of the gross features in the differential cross section may be attributed entirely to constraints of conservation of energy and momenta. A posteriori at least, the feasibility of estimating appropriate weighting functions is demonstrated.

$Rb + CH_3I$

The reaction of an alkali with CH_3I is an example of a repulsive interaction exhibiting backward ("rebound") scattering in which a substantial fraction of the reaction exothermicity is converted into translational energy.

Beuhler and Bernstein[21] have studied the reactive symmetry for this system caused by orienting the methyl iodide molecules. They find the $Rb\text{-}ICH_3$ orientation to be at least five times more reactive than the $Rb\text{-}H_3CI$ orientation. While we cannot make explicit use of this data to determine a weighting function, these results suggest a choice of n in the range 1-2 for the weighting function R_θ. Recent experiments[44]

indicate that the most probable E'_{trans} is large, probably about 15 kcal/mole, which for $Rb + CH_3I$ gives a most probable α of 15. Fig. 5 gives the results for n = 1, positive impulse (repulsive interaction), for α in the range 10 to 20. The calculated curves resemble the published experimental results[45] for this system. Because of the high value of α, the angular distributions are nearly independent of α. This result is in accord with the experimental finding[44] that the angular distribution is only weakly coupled to the energy distribution.[46]

$M + X_2$ - Trends

In this section the trends expected in the alkali halide systems are examined in order to compare with those observed in the angular distributions for $K + Cl_2$, Br_2 and I_2 by Grice and Empedocles[47] and for Li, Na, K, Rb, Cs + Br_2 by Parrish and Herm.[48]

For the X_2 systems we may use the model in its simplest form (i.e., employing a minimum amount of experimental information). Three parameters must be assigned: the sign of the impulse, the value of α and index n of the weighting function R_θ. The alkali-halogen reactions are known to be of the "attractive" type as evidenced by their extremely large cross sections, thus implying a negative impulse. The simplest assumption regarding the value of the most probable α is that the reactions are "collisionally thermoneutral," i.e., Q = 0, so that α is determined by mass factors alone. The resulting values of $\alpha(Q = 0)$ for $K + Cl_2$, Br_2 and I_2 may be found in Table 2.

The choice of weighting is only slightly more difficult. Some weighting is clearly indicated since configurations such as A-C-B, where A departs with B, should have considerably less weight than A-B-C. (Recall that even though B and C are here identical X atoms, the model distinguishes between B and C.) The form of the weighting function R_θ, i.e., the choice of the weighting parameter n is however, not extremely crucial, and a choice of $n = 1$ seems reasonable.

With these values for the model parameters the calculated angular distributions are shown in Fig. 6. They agree well with the experimental results of Ref. 47.

Since more detailed data exist for $K + Br_2$ and $K + I_2$ it is worthwhile to apply the model in its more flexible form to determine the "experimental" values for the sign of the impulse and weighting parameter by fitting the observed angular distributions using experimental values for α. For $K + Br_2$ the attempt is made to fit the angular distribution of Birely et al.,[49] folding in the product recoil energy distribution function of Warnock et al.[50] The product energy distribution is converted to a distribution over α at the nominal collision energy E. The optimum, fitted, value for the weighting parameter was found to be $n = 0.7$, with a negative impulse as anticipated. The differential cross section averaged over α is not extremely sensitive to n, but is, of course, very sensitive to the sign of the impulse. (Switching from negative to positive impulse shifts the products into the backward hemisphere.[51]) For $K + I_2$ complete flux-velocity-angle contour maps (product intensity as a function of angle and velocity) are available[52] for several E_{tr}.

The optimum parameters found by fitting the entire flux maps turn out to be the same as the above values for the K + Br_2 system.[53]

A negative impulse and a weighting parameter $n = 0.7$ are used for the Li, Na, K, Rb, Cs + Br_2 systems. The values of α used are those listed in Table 2. These calculations give similar angular distributions to those of Fig. 6. Table 1 lists the results as $\chi_{1/2}$, the width of the angular distributions $d^2\sigma_R(\chi)/d^2\omega$ at half-height, compared with the experimental $\chi_{1/2}$ values. The trend observed by Parrish and Herm[48] is found, supporting their assertion that the broadened LiBr angular distribution may be attributed to a "mass effect in the overall reaction dynamics."

Note that the present model has nothing to say about <u>how</u> the available energy is partitioned between product excitation and recoil energy, but <u>given</u> this partitioning, the kinematics require a broader angular distribution because of the small Li mass which results in a large value for α. Table 1 also shows that as the alkali mass increases the angular distribution becomes more peaked in the forward direction. However, the observed K, Rb, Cs + Br_2 angular distributions[49] appear to be virtually identical. Possibly the weighting index $n = 0.7$ should be decreased slightly for the larger atoms to permit more reaction configurations. This change would bring the calculated $\chi_{1/2}$ values for the K, Rb, and Cs systems closer together and have little effect on the Na and Li systems.

Table 1. Width at half-height, $\chi_{1/2}$, of the angular distributions, $d^2\sigma_R(\chi)/d^2\omega$, for the M + Br_2 reactions (peaked at $\chi = 0$)

M	$\chi_{1/2}$ (deg.) Model[a] Calc.	Exptl.[48]
Li	85	100
Na	70	70
K	60	60
Rb	55	60
Cs	35	60

[a] Model parameters: negative impulse, weighting index n = 0.7, α values from Table 2 .

K + HBr

The systems K + HBr, DBr were studied by Gillen et al.[54] Because of the pathological kinematics for these systems the derived c.m. angular distributions are quite uncertain and a meaningful determination of the model parameters by a fitting procedure cannot be made. One can say, however, that because the alphas are large [$\alpha \approx$ 11(K, HBr), 8 (K, DBr), and 7 (K, TBr)], very broad distributions are predicted unless the weighting parameter n is much greater than unity. (This seems unlikely considering the size of K and Br compared to hydrogen.) Angular distributions obtained from the model for any reasonable choice

of weights (with either positive or negative impulse) are found to agree qualitatively with the HBr and DBr data of Ref. 54, but predict that the KBr from the reaction with TBr should be peaked slightly more forward than for K + HBr or K + DBr. Unfortunately, this is contrary to the findings of Martin and Kinsey.[55] From Ref. 54 the energy distributions for the H- and K- systems are both broad, with the D- distribution slightly broader than that for H . If there were a considerable contribution to the T- distribution from higher E' (i.e., higher α), this discrepancy could be explained.[56]

B. Product Rotational Energy Distributions

Based on the analysis given in Appendix II, calculations have been made of the angular distribution of the average change in rotational angular momentum of product AB with respect to reactant BC. The quantity δ_{rot} given in Eq. (21) has been calculated for various scattering angles χ . For the systems chosen the values of the parameters r_{BC} , R (and g'/g) used are those listed in Table 3.

For the case of K + HBr, TBr, the calculations indicated that for both systems δ_{rot} was only weakly dependent on angle, declining with χ smoothly from a value of 1.1 at $\chi = 0°$ to 0.9 at $\chi = 180°$. Averaging δ_{rot} over angles, assuming an isotropic angular distribution of products, yields a quantity $\langle\delta_{rot}\rangle$ which is related to the average final rotational energy $\bar{E}'_{rot}$ by the following equation:

$$\bar{E}'_{rot} = \frac{\mu}{\mu'}\left[\frac{\langle\delta_{rot}\rangle}{4\pi}\frac{E_{tr}}{(r_{BC}/R)^2} + E_{rot}\right] . \qquad (25)$$

Here $\mathcal{I}$ and $\mathcal{I}'$ are, respectively, moments of inertia of BC and AB . For $E_{rot} \approx 0.15$ kcal/mole, $\bar{E}'_{rot}$ turns out to be 8.4 kcal/mole for K + HBr and 1.8 kcal/mole for K + TBr . For K + HBr, 8.4 kcal/mole exceeds the energy available for rotational excitation.[57] Equation (25) may be used to compute product rotational energy at specified angles by substituting δ_{rot} for $\langle\delta_{rot}\rangle$. Examination of the K + HBr results at each angle reveals that E'_{rot} exceeds 6.2 kcal/mole at every angle. The difficulty can be traced to the extremely sensitive dependence of E'_{rot} on the value of R while δ_{rot} is only very weakly dependent on the choice of R . A change in R from 3.34 to 2.5 modifies the δ_{rot} vs. χ plot imperceptibly but will reduce E'_{rot} to less than 6.2 kcal/mole at all angles ($\delta_{rot} = 1.40$ corresponds to $E'_{rot} = 6.2$ kcal/mole). Note, however, that a large value of E'_{rot} for K + HBr is expected because the mass ratio demands that[58] $\underset{\sim}{L} = \underset{\sim}{j}'$.

Because of this extremely critical dependence on R , which arises in converting angular momentum to rotational energy or vice versa, one attractive potential application of the model must be set aside. While general features of the E'_{rot} distribution (flat, peaked forward, etc.) are significant, no real significance may be attached to the absolute values of E'_{rot} . This precludes the possibility of invoking the conservation of energy to obtain constraints on the angular distribution of products, based on rotational excitation of the products.

Figure 7 presents the results δ_{rot} vs. χ for the systems Li, K, Cs + Br_2 . The behavior seen there is in general agreement with Kuntz et al.[30] who found a positive correlation between scattering angle

and enhancement of product rotational energy in their potential surface calculations for $K + Br_2$. These authors do not report a plot such as Fig. 7, but only a single number which is the correlation coefficient for rotational excitation and scattering angle. Our results indicate that the excitation function vs. χ is broad, slightly favoring the forward direction. This prediction is actually in closer agreement with the experimental study by Grice et. al.[59], who found that the reactively scattered RbBr from $Rb + Br_2$ could be characterized by the same rotational temperature at all angles for which they made observations. The most outstanding feature of Fig. 7 is the bimodal excitation function for LiBr. The bimodal distribution persists for a wide range of (g'/g) values and for $0.2 \leq r_{BC}/R \leq 1$. (Values of $r_{BC}/R > 1$ were not investigated.) $\bar{E}'_{rot}$, computed from Eq. (25), for Li, K, Cs + Br_2 is 0.5, 1.2, and 2.5 kcal/mole, respectively, with $E_{rot} = 0.6$ kcal/mole. If the angular distributions are taken into account in the average and considering that for $M + Br_2$, E'_{tr} (B) reported in Table 1 of Ref. 48 are probably too low, good agreement between the model and experiment[59,60] can be obtained.

Table 2. Summary of relevant experimental results from the literature.

	$\bar{E}$(kcal/mol)[a]	E'_{mp}(kcal/mol)	μ/μ'	α	$\chi_{1/2}$(deg)
Rb + CH_3I [b]	1.5	~ 15	3.81	15.3	90
Li + Br_2 [c]	2.0	6.6	0.160	9.09	100
Na + Br_2 [d]	1.28	5.2	0.447	6.03	70
K + Br_2 [e]	1.23	3.7	0.657	4.28 (2.47[f])	60
Rb + Br_2 [e]	1.01	2.8	1.03	3.28	60
Cs + Br_2 [e]	1.06	1.8	1.25	2.33	60
K + Cl_2 [g]	----	---	1.05	1.95 [f]	--
K + I_2 [g]	----	---	0.471	2.91 [f]	--
K + HBr [g,h]	2.8	1.5	26.6	11.5	--
K + DBr [g]	2.8 [i]	1.5 [i]	13.5	8.15	--
K + TBr [g]	2.8 [i]	1.5 [i]	9.08	6.70	--

a. Nominal value of average initial relative energy.

b. Estimated from unpublished results on K + CH_3I by A. M. Rulis and R. B. Bernstein

c. Ref. 48.

d. Ref. 61.

e. Ref. 49.

f. Alpha computed assuming $Q = 0$.

g. Data not entered if not referred to in text.

h. Ref. 54.

i. Assumed identical to K + HBr.

Table 3. Summary of parameters used in the calculations.

	$(g'/g)_{mp}$ [a]	r_{BC}(Å)	σ_R(Å^2)	R(Å)
K + HBr	3.77	1.41	35 [c]	3.34
K + TBr	2.21	1.41	35 [d]	3.34
Li + Br_2	0.726	2.3	115-146 [e]	~ 6.4
K + Br_2	1.41	2.3	220-260 [f]	~ 8.7
Cs + Br_2	1.46	2.3	370-380 [f]	~ 11

a. Computed by $(g'/g)_{mp} \simeq (\mu E'/\mu' E)^{1/2}$. The error resulting from using E_{mp} instead of g_{mp} is probably less than the uncertainties in the energies.

b. Ref. 62.

c. Ref. 54.

d. Assumed equal to that for K + HBr. This is in disagreement with expectations based on the K + HBr, DBr experiments,[54] where a significant difference in σ_R was found. However, it is believed that the difference observed is largely due to the quantal isotope effects which cannot properly be treated by the present model.

e. Ref. 48.

f. Ref. 49.

VI. CONCLUSIONS

A simple kinematic model for reactive collisions A + BC → AB + C has been developed which includes aspects of mass and momentum transfer and for which the equations of motion are readily soluble. Required as input are the masses of the particles, the initial and final translational energies, and a value for R , the distance between A and the c.m. of BC at which mass transfer occurs. Information on the potential surface is introduced via a weighting function for the direction of net momentum transfer, or alternatively reaction configurations, and by the sign (positive or negative) of the net momentum transfer. The model is formally equivalent to an impulsive model, yet because of the definition of net momentum transfer or impulse, it has greater generality. Attractive and repulsive systems may be treated. The model admits an analytical solution for the differential and total cross sections. No internal degrees of freedom are included so vibrational energy enters only as a parameter through the conservation of energy equation.

The differential reaction cross section exhibits a wide variation in shape depending on parameter values. By changing the initial and final energies, the masses, and the configuration weighting, it is possible to obtain broad or narrow distributions peaked forward, backwards (or even sidewards). The reactive scattering for Rb + CH_3I; M + X_2 ; and K + isotopic HBr molecules has been examined to determine if reasonable choices for the potential parameters can be made based on gross, "chemical" considerations.

One purpose in developing this model was to isolate those features of the differential reaction cross section which could be attributed mainly to kinematic constraints. To do this with a single model, a certain amount of adaptability must be added to the model by including parameters characteristic of the potential. The Rb + CH_3I example demonstrates that the model is applicable to repulsive as well as attractive systems. The model predicts only very weak coupling between the recoil energy (E'_{tr}) and the angular distributions, at least when α is large (as it is for Rb + CH_3I and the K + HBr series). For α near unity, significant coupling is predicted. For the M + X_2 series the trend in the angular distributions for K + Cl_2, Br_2, and I_2 has been established using the model in its crudest form. The assignment of the weighting parameter n was refined by choosing one system in the series (K + Br_2) as the touchstone and fitting the experimental results to optimize the parameter, and then predicting fairly well the trend found experimentally in the Li, Na, K, Rb, and Cs + Br_2 series. These calculations also confirm Parrish and Herm's[48] "mass" effect for Li. For the K + HBr series it is found, with little or no potential input, that a broad angular distribution of products is to be expected on kinematic grounds alone.

Generalized kinematic models should prove valuable in two respects: first, by providing a means for isolating features of reactive scattering which are dictated primarily by kinematics and thus allowing one to concentrate on those features directly related to particle interactions, and second, by providing a basis for understanding or predicting trends in a series of reactions involving similar species. Another possible applica-

tion would be to provide a convenient source for rapidly-calculated reactive trajectories which might be used in a semiclassical treatment of reactive scattering.

APPENDIX I: DERIVATION OF DIFFERENTIAL REACTION CROSS SECTION

In general terms one may view the "generalized differential reaction cross section" as a probability density $f(x)$ which is a function of a multidimensional variable x, and which is related to a distribution function $F(x)$ by $f(x) = dF(x)/dx$. The quantity dF then is the probability that the variable assumes a value in the range x and $x + dx$. For the reactive scattering problem x subsumes the variables b and β which are the impact parameter and azimuthal angle; θ and ϕ which are the target orientation angles; and χ and ψ which are the scattering angles. The infinitesimal element of probability is a six-dimensional quantity

$$d^6\sigma(\eta,\Upsilon,\omega) = d^2S(\eta)\,d^2G(\Upsilon)\,d^2H(\omega) \tag{I.1}$$

$$\eta \leftrightarrow b, \beta$$
$$\Upsilon \leftrightarrow \theta, \phi$$
$$\omega \leftrightarrow \chi, \psi.$$

where S, G, and H are two-dimensional distribution functions for the appropriate variables. In writing this equation it is implicitly assumed that the variables η, Υ, and ω are independent, which is not the case in general. However, quite often the coupling between sets is simple, so one can proceed with the independent formulation for clarity, incorporating coupling as it arises. It is worth emphasizing that all the dynamical information contained in the model pertinent to the scattering angle must be included in the distribution functions.

As an example consider the simple hard sphere (SHS) model in which T is a null set and b and χ are related uniquely. Equation (I.1) is simplified:

$$d^4\sigma_{SHS}(n,\omega) = d^2S(n)\, d^2H(\omega). \qquad (I.2)$$

Since b and β are to be integrated, we consider χ and ψ as dependent variables. The function S is not a distribution function in the usual sense since it is "extensive" with a maximum value of $2\pi R^2$ which comes from $b^2\beta$. (This distribution is therefore not normalized to one.) The differential cross section for this model is

$$d^4\sigma_{SHS}(n,\omega) = P_{b'} P_\beta b' db d\beta P_\chi P_\psi \delta[\chi_b - \chi_{b'}]\, \delta[\psi-\beta]\, \frac{\sin\chi_b}{\sin\chi_{b'}}\, d\chi d\psi. \qquad (I.3)$$

The P functions are weighting functions which contain the rest of the model information not explicitly contained in (I.3). In this case they are all unity except for P_b , which is a step function with value 1 for $b \leq R$ and zero for $b > R$. The delta functions arise because the relationship $\chi_b = 2\cos^{-1}(b/R)$ establishes a one-to-one correspondence between χ and b and $\psi = \beta$ because all forces are impulsive. The primed b's are the problem variables, the unprimed b's are functional (dummy) variables. The normalization for H is determined by $N\int\int\delta(\psi-\beta)\delta(\chi_b - \chi_{b'})\sin\chi_b d\chi d\psi = 1$, where b' and β are independent variables. The distribution function H may also be written such that $d^2H(\omega) = \delta(\psi-\beta)\delta[\cos\chi_b - \cos\chi_{b'}]d(\cos\chi_b)d\psi$.

The integration over β is easily performed and serves to remove the function $\delta(\psi-\beta)$. To perform the integration over b' the independent variable must be made explicit in the function $\delta(\chi_b-\chi_{b'})$. This can be accomplished by using the identity

$\delta[g(\chi)] = \Sigma|g'(\chi_i)|^{-1}\cdot\delta(\chi-\chi_i)$, where χ_i are the roots $g(\chi_i) = 0$. For this model there is a single root $b = b'$ and Eq. (I.3) becomes

$$d^2\sigma_{SHS}(\omega) = \int_0^R b'db' \left|\frac{d\chi}{db}\right|^{-1}_{b=b'} \delta[b-b'] \frac{\sin\chi_b}{\sin\chi_{b'}}\, dx\, d\psi \qquad (I.4)$$

which gives the well-known result

$$d^2\sigma_{SHS}(\omega) = b\left|\frac{db}{d\chi}\right| \frac{\sin\chi}{\sin\chi}\, d\chi\, d\psi \qquad (I.5)$$

or

$$\frac{d^2\sigma_{SHS}}{d^2\omega} = \frac{b}{\sin\chi}\left|\frac{db}{d\chi}\right| . \qquad (I.6)$$

The subscript b has been suppressed since it is now redundant. Equation (I.6) is the well-known SHS result. Upon inserting the relation between b and χ, one finds $d^2\sigma_{SHS}/d^2\omega = R^2/4$.

The general result, including $G(T)$, is

$$d^6\sigma(\eta, \Upsilon, \omega) = P_\eta\, d^2\eta\, P_\Upsilon\, d^2\Upsilon\, P_\omega\, d^2\omega , \qquad (I.7)$$

where the P's must be determined from the model under study. The order of Eq. (I.7) may be increased by including distribution functions for

translational and/or internal energy. In keeping with the goal of deriving a simple model these possibilities are ignored. One must examine next the coupling between η, T and ω. In the present model, the probability that a certain reaction occurs yielding products in ω to $\omega + d\omega$ when the target has an orientation in T to $T + dT$, does not depend on impact parameter. Separability does not obtain when configuration weighting functions are used which depend on the impact parameter. This situation is discussed in the section on configuration weighting where the net result of including such weighting is to produce a constant factor which may be included in $G(T)$. Coupling between ω and T will always exist for any model in which target orientation plays a role in the angular distribution of products. In the present deterministic model there exists a one-to-one relation between (θ,ϕ) and (χ,ψ) which may be expressed as delta functions $\delta(\chi_\theta - \chi_{\theta'})$ and $\delta(\phi-\psi)$. The theta subscript on χ_θ indicates the choice of χ as the dependent variable where $\cos\chi_\theta$ is given by Eq. (12') in the text. Equation (I.7) may be expanded as follows

$$d^6\sigma = P_b P_\beta b\,db\,d\beta P_{\theta'} P_{\phi'} \frac{\sin\theta'}{4\pi} d\theta' d\phi' \delta[\phi'-\psi]\,\delta[\chi_\theta - \chi_{\theta'}] \frac{\sin\theta}{\sin\chi_{\theta'}} dx\,d\psi, \qquad \text{(I.8)}$$

where P_β and $P_{\phi'}$ can be taken as 1, P_b may be chosen as the step function discussed above and $P_{\theta'}$ is a configuration weighting function normalized so $\int P_{\theta'} \sin\theta' d\theta' = 2$. Since the scattering is independent of the laboratory coordinates the differential cross section depends only on $\beta - \phi'$ and not β and ϕ', so that a change of variables to

$\phi = \phi' - \beta$ and $\beta = \beta$ is warranted. The following integrations may be performed: (1) over b which gives a factor $R^2/2$; (2) over β which removes $\delta(\phi-\beta-\psi)$; (3) and over ϕ which yields a factor 2π . Collecting terms Eq. (I.8) becomes

$$d^3\sigma(\theta',\omega) = \frac{\sigma}{4\pi} P_{\theta'} \sin\theta' d\theta' \delta[\chi_\theta - \chi_{\theta'}] \frac{\sin\chi_\theta}{\sin\chi_{\theta'}} dx\, d\psi. \qquad \text{(I.9)}$$

To perform the integration over θ' the independent and dependent variables in $\delta[\chi_\theta - \chi_{\theta'}]$ must be interchanged. This transformation can be accomplished by using the relation mentioned above and Eq. (I.9) becomes

$$\frac{d^2\sigma}{d^2\omega} = \sigma \frac{P_\theta(\theta_\chi)}{4\pi \sin\chi} \left|\frac{d\cos\theta}{d\chi}\right|_{\theta=\theta_\chi}, \qquad \text{(I.10)}$$

which upon substituting Eq. (12) of the text yields

$$\frac{d^2\sigma}{d^2\omega} = \sigma \frac{P_\theta(\theta_\chi)}{4\pi} \frac{\alpha^2 |(\alpha - \cos\chi)|}{[1 - 2\alpha\cos\chi + \alpha^2]^{3/2}}. \qquad \text{(I.11)}$$

This is the "working formula", Eq. 18 of the Sec. III.B.

The differential cross section including out-of-plane contributions may be obtained from (I.11) by integrating over ψ to give

$$\frac{d\sigma}{d\chi} = \frac{\sigma}{2} P_\theta \frac{\alpha^2 |(\alpha - \cos\chi)| \sin\chi}{[1 - 2\alpha\cos\chi + \alpha^2]^{3/2}}. \qquad \text{(I.12)}$$

APPENDIX II. ROTATIONAL ENERGY CHANGE AS A FUNCTION OF SCATTERING ANGLE

In this appendix Eq. (2) of Sec. II is solved to find the final rotational angular momentum j'. Once the scattering angle and reaction configuration are specified, Eq. (2) may be solved for $\underset{\sim}{j}'$. Note that Eq. (2) is a vector equation, implying three independent relationships and there are three unknowns corresponding to the components of $\underset{\sim}{j}'$. This appendix is restricted to finding only the magnitude of $\underset{\sim}{j}'$ as a function of χ.

The computation begins by defining the following vectors for a given collision configuration: $\underset{\sim}{R}$, from A to the c.m. of BC, $\underset{\sim}{r}$ from C to the c.m. AB; and $\underset{\sim}{r}_{BC}$ from B to C, along the bond axis. The orbital angular momentum vectors are written

$$\underset{\sim}{L} = -\mu(\underset{\sim}{R} \times \underset{\sim}{g}) \quad \text{and} \quad \underset{\sim}{L}' = \mu'(\underset{\sim}{r} \times \underset{\sim}{g}'), \tag{II.1}$$

where $\mu = A(B + C)(A + B + C)^{-1}$, $\mu' = (A + B)C(A + B + C)^{-1}$, and the signs are different because of the definition of $\underset{\sim}{g} = \underset{\sim}{w}_A - \underset{\sim}{w}_{AB}$ and $\underset{\sim}{g}' = \underset{\sim}{w}_{AB} - \underset{\sim}{w}_C$. Specification of $\underset{\sim}{r}$ and $\underset{\sim}{R}$ requires knowledge of the impact parameter. The vector $\underset{\sim}{R}$ is defined in terms the angle $\gamma = \sin^{-1}(b/R)$ by

$$\underset{\sim}{R} = R(\sin\gamma, 0, \cos\gamma), \tag{II.2}$$

and $\underset{\sim}{r}$ is found to be

$$\underset{\sim}{r} = -A(B+C)^{-1}\underset{\sim}{R} - B(A+B+C)[(A+B)(B+C)]^{-1}\underset{\sim}{r}_{BC}. \tag{II.3}$$

The explicit forms for $\underset{\sim}{g}$ and $\underset{\sim}{g}'$ are required for computation and are given by

$$\underset{\sim}{g} = g(0,0,1) \tag{II.4}$$

and

$$\underset{\sim}{g}' = g'(\sin\chi\cos\psi, \sin\chi\sin\psi, \cos\chi), \tag{II.5}$$

where ψ is the azimuthal angle for the scattered products. Note for this model it is easily shown that $\psi = \phi$. Since only magnitudes are required, Eq. (2) may be squared and written

$$j'^2 - j^2 = L^2 - 2\,\underset{\sim}{L}\cdot\underset{\sim}{L}' + L'^2 . \tag{II.6}$$

The cross term $\underset{\sim}{j}\cdot(\underset{\sim}{L} - \underset{\sim}{L}')$ has been dropped in Eq. (II.6) because, while it is non-zero, $\underset{\sim}{L}$ and $\underset{\sim}{L}'$ do not depend on $\underset{\sim}{j}'$ and the cross term will vanish when the average is taken over all angles $\hat{\underset{\sim}{j}}$. Expanding (II.6), using the definitions above, one obtains

$$\begin{aligned} j'^2 - j^2 = {} & (\mu g R)^2 \sin^2\gamma - 2(\mu' g')(\mu g R \sin\gamma)\times \\ & \left[(\rho\cos\gamma + \bar{\rho}\cos\theta)\sin\chi\cos\psi - \cos\chi(\rho\sin\gamma + \bar{\rho}\sin\theta\cos\phi)\right] \\ & + (\mu' g')^2\Big\{\rho^2 + \bar{\rho}^2 + 2\rho\bar{\rho}(\sin\gamma\sin\theta\sin\phi + \cos\gamma\cos\theta) \\ & - \left[\rho(\sin\gamma\sin\chi\cos\psi + \cos\gamma\cos\chi)\right. \\ & \left. + \bar{\rho}(\sin\theta\sin\chi\cos(\phi-\psi) + \cos\theta\cos\chi)\right]^2\Big\}, \end{aligned} \tag{II.7}$$

where

$$\rho \equiv -A(A+B)^{-1}R \quad \text{and} \quad \bar{\rho} \equiv -B(A+B+C)[(A+B)(B+C)]^{-1}r_{BC}.$$

Equation (II.7) may now be averaged over all b, ϕ, and ψ to obtain the angular momentum difference:

$$\langle j'^2 - j^2 \rangle_{b,\phi,\psi} = \frac{1}{2\pi^2}\int_0^{\pi/2} d\gamma \sin\gamma\cos\gamma \int_0^{2\pi} d\phi \int_0^{2\pi} d\psi\ \delta(\phi-\psi)[j'^2 - j^2], \quad \text{(II.8)}$$

The variable θ is an implicit function of χ and is therefore not averaged. When the integrations in (II.8) are performed the following result is obtained:

$$\langle j'^2 - j^2 \rangle = \frac{(\mu g R)^2}{4\pi}\left\{1 + 2f(g'/g)\cos\chi + (g'/g)^2\left[f^2 + \tfrac{1}{2}f^2\sin^2\chi\right.\right.$$

$$\left.\left. + \frac{8}{3}\left(\frac{r_{BC}}{R}\right)\frac{BC^2(A+B+C)}{A(B+C)^3}\sin\chi\sin(\chi-\theta) + 2\left(\frac{r_{BC}}{R}\right)^2\frac{B^2C^2(A+B+C)^2}{A^2(B+C)^4}\sin^2(\chi-\theta)\right]\right\}, \quad \text{(II.9)}$$

where $f = C(B + C)^{-1}$. This equation is used to compute the results discussed in Sec. V.2.

APPENDIX III. LOADED-HARD-SPHERE MODEL

The first model derived as an improvement over the simple hard-sphere model for reactive collisions[19] was a model based on the concept of loaded-hard-spheres (LHS). A diagram displaying a reaction configuration for reactants and defining certain vector quantities is displayed in Fig. III.1.

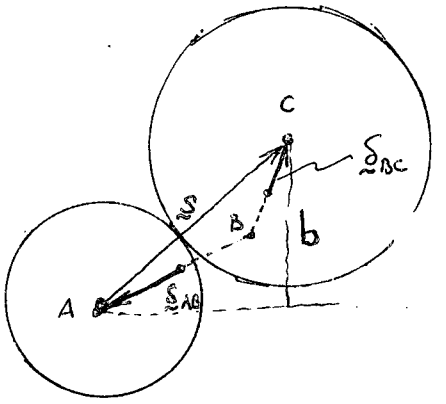

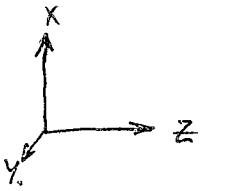

c.m. coordinate system orientation located at c.m. A-B-C

Fig. III.1 Reaction configuration for A + BC. The symbols A, B, and C represent the atomic species undergoing reaction A + BC → AB + C .

In this figure $\underset{\sim}{\delta}_{BC}(\underset{\sim}{\delta}_{AB})$ is the vector from the c.m. of BC(AB) to C(A) and $\underset{\sim}{S}$ is a vector between the centers of the two spheres. Initially the BC-sphere is loaded; after reaction new spheres may be envisioned having the same centers and the same sum of radii but with appropriate radii so that AB is now loaded and the load is within the AB sphere. The load may appear out of the plane of the page and its orientation is defined by (θ,ϕ) as defined in Fig. 1 in the main text.

The conservation equations Eqs. (1)-(3) apply and the initial velocity $\underset{\sim}{g}$ is taken to lie in the positive z-direction. The model definition is completed by defining values for three of the ten unknowns in the conservation equations. We assume that the momentum transfer occurs as it does for hard spheres, along the line of centers, i.e., the impulse direction is

$$\hat{\underset{\sim}{I}} \equiv \underset{\sim}{I}/I = \underset{\sim}{S}/S \quad . \tag{III.1}$$

For the third variable we assume that the final translational energy E'_{trans} is known or that $|\underset{\sim}{g}'|$ is specified.

The differences between the LHS model and the model developed in the main text (MB model) are that the atom C is at the center of the BC-sphere and the direction of the impulse is defined differently. The LHS includes an attempt to couple the rotational and orbital angular momentum $\underset{\sim}{j}$ and $\underset{\sim}{L}$. When a loaded sphere with non-zero $|\underset{\sim}{j}|$ travels through space it will wobble because it rotates about its own c.m. While coupling these variables is an admirable intention it complicates the solution of the equations and is probably not worthwhile. In contrast to the MB model the LHS model requires the specification of impact parameter, b, to determine the scattering angle χ. As can be seen from Fig. III.1, because the c.m. of BC does not lie at the center of the sphere, the range of impact parameters is a function of $\underset{\sim}{\delta}_{BC}$. This has at least two unpleasant consequences: (1) the limits of integration for averaging over configuration are messy, and (2) for those configurations in which the BC c.m. lies above the yz-plane, the function $\chi = \chi(b)$ is double-valued and a rainbow is produced.[63]

The derivation of the LHS equations follows closely the MB derivation. Equation (10) is valid here; Eq. (11) is written

$$\alpha \cos\chi + (I/fp)\left(\hat{\underset{\sim}{I}}\right)_z = 1, \qquad \text{(III.2)}$$

where $(\hat{\underset{\sim}{I}})z$ is the z-component of $\hat{\underset{\sim}{I}}$. The quantity $(\hat{\underset{\sim}{I}})z$ is identical in the two models

$$\left(\hat{\underset{\sim}{I}}\right)_z = (1-\alpha\cos\chi)/(1-2\alpha\cos\chi+\alpha^2)^{1/2}. \qquad \text{(III.3)}$$

Up to this point the two models agree except that $(\underset{\sim}{I})_z$ cannot be less than zero for the LHS. From this point the models diverge, the remaining components of $\underset{\sim}{I}$ are different and the differential cross section is constructed differently.

Equations (10), (III.1), and (III.2) and the definition for $\underset{\sim}{I}$ may be used to find the scattering angle as a function of b depending on (θ,ϕ)

$$\chi = \chi(b;\theta,\phi). \qquad \text{(III.4)}$$

However, this is not the desired quantity to determine the differential cross section, rather χ must be the independent variable and b must be known as a function of χ

$$b = b(\chi;\theta,\phi). \qquad \text{(III.5)}$$

From Fig. (III.1) and Eq. (III.3) one obtains the following equation

$$S^2\left(\hat{\underset{\sim}{I}}\right)_z^2 = S^2 - \left[(\underset{\sim}{\delta}_{BC})_x + b\right]^2 - (\underset{\sim}{\delta}_{BC})_y^2 \qquad \text{(III.6)}$$

which gives a quadratic equation in b with the solution

$$b = -\left(\underset{\sim}{\delta}_{BC}\right)_x \pm \left\{ \frac{(\alpha S \sin\chi)^2}{(1-2\alpha\cos\chi+\alpha^2)} - \left(\underset{\sim}{\delta}_{BC}\right)_y^2 \right\}^{1/2}, \tag{III.7}$$

where

$$\underset{\sim}{\delta}_{BC} = \delta_{BC}\left(\sin\theta\cos\phi, \sin\theta\sin\phi, \cos\theta\right). \tag{III.8}$$

The positive root is always valid; the negative root is also valid (i.e., there exist two b's for the same χ) when $\chi < \chi_0$ and $\phi > 90°$. The quantity χ_0 is defined by setting $b = 0$ in Eq. (III.7) and solving for χ,

$$\alpha\cos\chi_0 = D - \left[(D-1)(D-\alpha^2)\right]^{1/2}, \tag{III.9}$$

where $D \equiv (\delta_{BC}\sin\theta/S)^2$. Also when $\phi > 90°$, a rainbow is produced at χ_r determined by

$$\alpha\cos\chi_r = F - \left[(F-1)(F-\alpha^2)\right]^{1/2}, \tag{III.10}$$

Where $F \equiv (\delta_{BC}\sin\theta\sin\phi/S)^2$. The quantity χ_r is only defined for $\phi > 90°$; for $\phi \leq 90°$, $\chi_r = \chi_0$. Because of the LHS condition $(\hat{\underset{\sim}{I}})z \geq 0$, Eq. (V.3) implies that for $\alpha > 1$ there exists a minimum scattering angle $\chi_m > 0$. This condition for $\alpha > 0$ and $\alpha < 0$ may be written,

$$\cos\chi_m = \min(1, 1/\alpha). \tag{III.11}$$

These conditions on the range of χ may be summarized schematically as

$$\chi_m(\alpha) \xrightarrow{\text{1 branch}} \chi_0(\theta) \xrightarrow{\text{2 branches}} \chi_r(\theta,\phi) \tag{III.12}$$

where the range $\chi_0 \rightarrow \chi_r$ is zero if $\phi \leq 90°$.

The differential cross section for the LHS model may be found by using the standard formula[64]

$$\frac{d^2\sigma}{d^2\omega} = \sum_{\text{branches}} \frac{b}{\sin\chi} \left| \frac{db}{d\chi} \right| . \qquad \text{(III.13)}$$

Differentiating Eq. (V.7) with respect to χ and substituting with (III.13), one obtains

$$\frac{d^2\sigma}{d^2\omega} = \left(\frac{d^2\sigma_{RP}}{d^2\omega}\right)\left\{ \mathcal{H}(\chi-\chi_m)\mathcal{H}(\chi_r-\chi) \cdot \right.$$

$$\left. \left[1 - (\underset{\sim}{\delta}_{BC})_x/G - \mathcal{H}(\chi-\chi_0)\left(1 + (\underset{\sim}{\delta}_{BC})_x/G\right)\right]\right\}, \qquad \text{(III.14)}$$

where $d^2\sigma_{RP}/d^2\omega$ is given in Ref. 19.

$$\frac{d^2\sigma_{RP}}{d^2\omega} = (\alpha S)^2 \left\{ \frac{(\alpha\cos\chi - 1)(\cos\chi - \alpha)}{\left[(\alpha\cos\chi - 1) + \alpha(\cos\chi - \alpha)\right]^2} \right\}, \qquad \text{(III.15)}$$

G is defined

$$G \equiv \left[\frac{(\alpha S \sin\chi)^2}{(1 - 2\alpha\cos\chi + \alpha^2)} - (\underset{\sim}{\delta}_{BC})_y^2 \right]^{1/2},$$

and $\mathcal{H}$ is the heaviside function which has a value of 1 for positive arguments and zero for negative arguments.

To obtain the final differential cross section, Eq. (III.13) must be averaged over θ and ϕ. This requires dividing θ and ϕ into ranges and using limits which are themselves variables of the outer integration. When this is done[65] and the integrations are carried out, one obtains the far-from-obvious result that

$$\frac{d^2\sigma_{LHS}}{d^2w} = \frac{d^2\sigma_{RP}}{d^2w} \,. \qquad \text{(III.16)}$$

Needless to say, this is somewhat of a disappointment!

The LHS model is considerably more detailed than the simple RP model[19], and thus offers the possibility of more detailed information. For example, the final rotational energy as a function of χ may be calculated as we have done for the MB model. The calculation is not reproduced here (it is more complicated than the MB calculation), however, the results are qualitatively the same as those presented in the main text for the MB model. A second aspect of the model's detail is the possibility for weighting collisions according to impact parameter and/or configuration. When weighting is included the differential cross section will depart from the simple RP result. Several weighting functions were examined but the findings were discouraging. For all weighting functions based on configuration, backward scattering is still found and the shape of the angular distribution is not radically different from the distribution without weighting. Weighting based on b yields the same result unless large impact parameters are weighted more heavily than small ones, in which case the scattering shifts forward to side-scattering. It was not possible to obtain forward scattering. This model was therefore abandoned in favor of the MB model.

APPENDIX IV. POSSIBLE MODEL MODIFICATION

The model which has been described is in reality a family of models. The original goal was to find a classical model for which the equations of motion admit an analytical solution. This has led to the present impulsive model in which the net interaction between the reactants and products is compressed into an instantaneous momentum and mass transfer. The direction and magnitude of the momentum transfer governs the predictions of the model. The impulse assumption permits the equations of motion (or, equivalently, the conservation equations) to be solved exactly. A loaded-hard-spheres model was examined first since this is the simplest conceivable impulsive model. In this model the momentum transfer is constrained to occur along the line-of-centers at collision. When this proved unsatisfactory the strict hard-sphere concept was abandoned in favor of a reaction sphere determining the point at which reaction occurs and the direction of momentum transfer was assumed to depend on the collision configuration. The concept and meaning of weighting the collision configuration was introduced and discussed. It is clear that there is a great deal of leeway here in the development of a model. Weighting schemes quite different from the ones suggested here can easily be implemented and different criteria for direction of the impulse is also possible. In order to solve the equations of motion it was assumed that the final translational energy was known. One could equivalently specify the final vibrational or rotational energy and obtain the final trajectories uniquely. An alternative assumption is to assume

that the magnitude of the impulse is known which would then determine a final translational energy distribution. A model which assumes that the impulse is known and is constant for all collision configurations has been developed by Kuntz.[30]

Many additional refinements may be included which still provide an exactly soluble model. Two refinements (which have not been explored in depth), directed at improving the final rotational energy distribution, are (1) to consider the "spheres" rough so that there is a torque perpendicular to the collision axis (this would couple the orbital and rotational angular momentum), and (2) introduce the assumption of a "breathing sphere," i.e., define a reaction radius R which is a function of the collision configuration.

For any real system undergoing reaction, the products are not produced with one single final translational energy E' but rather with a distribution of final energies which is in general coupled to the scattering angle. In order to model a real system, a final energy distribution $P(E')$ or equivalently, if the initial energy is specified, a distribution $P(\alpha)$, must be guessed (based on say, statistical and quantum mechanical consideration) or determined experimentally and then folded into the angular distribution. An assumption commonly made in this regard is that the angular and energy distribution are uncoupled. In the present model this assumption is not involved since the angular distribution Eq. (18) depends explicitly on α. The actual dependence of χ_0 on α is weak, and can easily be modified in one of two ways: either directly by folding in a $P(\alpha,\chi)$ which depends explicitly on χ

or indirectly by choosing a weighting function $p(\theta,\alpha)$ which depends on α . Such ad hoc "refinements", however, only serve to weaken the value of a model as a predictive tool. They have therefore been disregarded.

APPENDIX V. $H + Cs_2$

An interesting case for application of the model is suggested by the recent study of the $H + Cs_2$ reaction by Lee, Gordon and Herschbach (LGH).[66] They have approximate results (no velocity analyses were performed) which indicate the differential reactive cross section is peaked in the sideways direction with a half width of $\sim$ 25°-45°; that it is not very sensitive to changes in the initial energy of the reactants; and that the most probable final energy is $\sim$ 1 kcal/mole. Their analysis suggested that the H atom has a high probability of attacking Cs_2 "from the side", causing the anisotropy in the angular distribution. Taking a cue from their mechanistic model one should weight most heavily those configurations in which Cs_2 is perpendicular to the H approach vector. (This is a naive abstraction in terms of their rather detailed mechanism involving short range HCs - Cs repulsion and long range HCs - Cs attraction. However, it seems reasonable to suppose the most probable direction of the net impulse is perpendicular to the approach vector if this is also the most probable approach.)

The weighting function chosen to emphasize the sideways attack was $\sin^n\theta$. Because of the high symmetry[67] of this function there is no change in scattering when the impulse changes sign so that we are searching for a one parameter description (n) of the angular distribution (given now, the form of the weighting function and α) .

As n increases from zero to one the angular distribution $d^2\sigma/d^2\omega$ moves from predominently forward scattering to a broad, skewed distribution peaking at 60° with a half width of 110°. If the weighting

is increased to $n = 6$ the distribution peaks at 75° with a half-width of 50°. As n is increased further the distribution remains stationary but continues to narrow. To shift the distribution back toward 90°, alpha must be increased. A good fit is obtained for $n = 6$. The fact that the distribution peaks at 75° is not inconsistent with the data reported by LGH. A relatively high value of n is required to give such a narrow angular distribution. It may also be significant that the wings of the angular distribution change from a convex curvature to concave, gaussian-like curvature only for $n \geq 2$.

The model also predicts, in accord with LGH, that the distribution should not significantly change in shape or position as the temperature of the reactants is increased. For $n = 6$, a change of alpha from three to twenty shifts the distribution from 65° to 85° and only narrows it slightly. Similar results may also be obtained with the model using $(1 + \cos\theta)^n$ weighting with positive impulse for $n \sim 0.5$. This distribution, however, is considerably broadened and for this weighting the model predicts a strong temperature dependence of the position and breadth of the distribution. Improved experimental information could easily distinguish between these two situations.

REFERENCES

1. For a review of (a) recent experimental developments in reactive scattering, see J. L. Kinsey, chapter in International Review of Science: Reaction Kinetics, MTP, Oxford (1972); (b) recent advances in chemiluminescence, see T. Carrington and J. C. Polanyi, chapter, ibid.; (c) recent developments in lasers in chemistry, see C. B. Moore, Ann. Rev. Phys. Chem. 22, 387 (1971).

2. For a review of theoretical-computational developments in reactive scattering, see R. D. Levine, chapter in International Review of Science: Theoretical Chemistry, MTP, Oxford (1972).

3. For a review of classical trajectory calculations see D. L. Bunker, Methods. Comput. Phys. 10, 287 (1971).

4. Statistical models have been discussed by (a) J. C. Light, Disc. Far. Soc. 44, 14 (1967). See also (b) E. E. Nikitin, Theor. Expt'l. Chem. 1, 83, 90 (1965) and (c) D. G. Truhlar, J. Chem. Phys. 54, 2635 (1971).

5. For a review of ion-molecule reaction models see A. Henglein, chapter in C. Schlier, Ed., Molecular Beams and Reaction Kinetics, Academic Press, N. Y. (1970), p. 139.

6. J. O. Hirschfelder and E. Wigner, J. Chem. Phys. 7, 616 (1939).

7. (a) H. M. Hulburt and J. O. Hirschfelder, J. Chem. Phys. 11, 276 (1943); for corrections to and extensions of this work see also (b) K. T. Tang, B. Kleinman, and M. Karplus, ibid. 50, 1119 (1969); (c) D. J. Diestler, ibid. 50, 4746 (1969); (d) P. D. Robinson, ibid. 52, 3175 (1970); (e) D. R. Dion, M. B. Milleur, and J. O. Hirschfelder, ibid. 52, 3179 (1970).

8. J. O. Hirschfelder, H. Eyring and B. Topley, J. Chem. Phys. 4, 170 (1936).

9. J. L. Magee, J. Chem. Phys. 8, 687 (1940).

10. W. F. Libby, J. Amer. Chem. Soc. 69, 2523 (1947).

11. P. J. Estrup and R. Wolfgang, ibid. 82, 2665 (1960).

12. R. J. Cross, Jr. and R. Wolfgang, J. Chem. Phys. 35, 2002 (1961).

13. Z. B. Alfassi and S. Amiel, Israel J. Chem. 7, 347 (1969).

14. (a) J. C. Light and J. Horrocks, Proc. Phys. Soc. (London) 84, 527 (1964); (b) C. Hsiung and A. A. Gordus, J. Amer. Chem. Soc. 86, 2782 (1964); J. Chem. Phys. 41, 1595 (1964).

15. M. Baer and S. Amiel, (a) J. Amer. Chem. Soc. 91, 6547 (1969); (b) Israel J. Chem. 7, 341 (1969).

16. R. H. Fowler and E. A. Guggenheim, Statistical Thermodynamics, Cambridge University Press, N. Y. (1939), p. 506.

17. R. D. Present, Proc. Natl. Acad. Sci. (U.S.) 41, 415 (1955).

18. R. D. Levine, Quantum Mechanics of Molecular Rate Processes, Oxford Press, London (1969), Chs. 3 and 4.

19. M. T. Marron, J. Chem. Phys. 52, 4060 (1970).

20. D. R. Herschbach, Adv. Chem. Phys. 10, 319 (1966).

21. (a) R. J. Beuhler, Jr. and R. B. Bernstein, J. Chem. Phys. 51, 5305 (1969); (b) R. J. Beuhler, Jr., Ph.D. thesis, University of Wisconsin (1968); Theoretical Chemistry Institute Report WIS-TCI-326X (1968).

22. (a) R. Grice, Mol. Phys. 19, 501 (1970); (b) R. Grice and D. R. Hardin, Mol. Phys. 21, 805 (1971).

23. (a) S. T. Butler, Proc. Roy. Soc. (London) A208, 559 (1951); (b) B. C. Eu, J. H. Huntington and J. Ross, Can. J. Phys. 49, 966 (1971).

24. R. E. Minturn, S. Datz, and R. L. Becker, J. Chem. Phys. 44, 1149 (1966).

25. (a) Z. Herman, J. Kerstetter, T. Rose, and R. Wolfgang, ibid. 44, 123 (1967);

(b) for a calculation employing this model to examine isotope effects see J. C. Light and S. Chan, J. Chem. Phys. 51, 1008 (1969).

26. D. T. Chang and J. C. Light, J. Chem. Phys. 52, 5687 (1970).

27. P. J. Kuntz, E. M. Nemeth, and J. C. Polanyi, J. Chem. Phys. 50, 4607 (1969).

28. D. D. Parrish and R. R. Herm, J. Chem. Phys. 53, 2431 (1970).

29. (a) R. J. Suplinskas, ibid. 49, 5046 (1968); (b) T. F. George and R. J. Suplinskas, ibid. 51, 3666 (1969); ibid. 54, 1037, 1046 (1971).

30. (a) P. J. Kuntz, M. H. Mok, and J. C. Polanyi, ibid. 50, 4623 (1969); (b) P. J. Kuntz, Ph.D. thesis, University of Toronto (1968); (c) P. J. Kuntz, Chem. Phys. Lett. 4, 129 (1969); (d) P. J. Kuntz, Trans. Far. Soc. 66, 2980 (1970); (d) P. J. Kuntz, Report WIS-TCI-468.

31. The Wolfgang-Chang-Light model has a great deal in common with that of Suplinskas (Ref. 29a) and the DIPR model of Kuntz (Ref. 30). Kuntz et al. present their model in terms of repulsive forces between C and AB which appears to be the opposite of Wolfgang's attractive forces model. However, as discussed in Ref. 32, the DIPR model may be viewed as a pseudo-hard-sphere model in which the impulse is the net force integrated over all time. This fact coupled with the possibility of changing the sign of the impulse permits one to view the DIPR model in "repulsive" or "attractive" terms or a mixture of both.

32. M. T. Marron, to be published.

33. D. R. Herschbach (private communication) has recently developed a model for a large variety of reactions, which uses the DIPR model with a simple recipe for specifying the magnitude of the impulse from data obtained either from photodissociation spectra or in some cases from electron attachment or collisional ionization experiments.

34. The first such study involving both velocity selection and analysis was that of (a) A. E. Grosser, A. R. Blythe and R. B. Bernstein, J. Chem. Phys. 42, 1268 (1965); recent, detailed investigations include that of (b) K. T. Gillen, A. M. Rulis and R. B. Bernstein, ibid. 54, 283 (1971) and (c) J. B. Cross and N. C. Blais, ibid. 55, 3970 (1971).

35. Appendix III contains a discussion of a loaded-hard-sphere model.

36. Although the impulse has thus far been considered to be directed along the B-C bond axis, this is not a necessary part of the model. The angular distribution of products does not depend on this unless a weighting function for the impulse orientation is used which depends explicitly on the molecular orientation. Only for the evaluation of the product rotational-energy distribution is the relationship between molecular orientation and impulse orientation required.

37. P. J. Kuntz, E. M. Nemeth, J. C. Polanyi, S. D. Rosner and C. E. Young, J. Chem. Phys. 44, 1168 (1966).

38. This relationship is not immediately obvious, but it may be inferred from the following discussion centered on the fate of the C atom, travelling along with B until "collision", at which point it receives

an impulse $\underset{\sim}{I}$ (in the direction θ,ϕ) and its trajectory is suddenly altered according to the conservation equations. For the case $\alpha > 1$, in a nearly head-on collision ($\theta \lesssim 0$), A approaches the B-end of the molecule; at collision, mass transfer occurs and C returns in the direction from which it approached, and AB is backscattered, i.e., $\chi > \pi/2$. This is easily interpreted as B-C repulsion. If the sign of $\underset{\sim}{I}$ is changed, C will continue along in its original direction and AB is forward-scattered. This may be interpreted as an attractive acceleration of BC by A in the entrance channel to such an extent that whatever the interactions in the reaction region and exit channel, C has developed sufficient momentum to continue on in the same direction. When $\alpha \leq 1$ the situation is complicated by the fact that a given configuration (θ,ϕ) can produce scattering at two angles depending upon the magnitude of $\underset{\sim}{I}$. Taking again the collinear case ($\theta = 0$), C is scattered both backward as above <u>and</u> forward. This is so because two vector diagrams are possible which will satisfy Eq. (6), one which is that of Fig. 1a where I is small (yielding $\chi < \pi/2$); and the other, for which I must be large can yield $\chi > \pi/2$. The former corresponds to a "glancing blow" which nevertheless involves B-C repulsion ($I > 0$) but only enough to "slow" $f\underset{\sim}{p}$ to $\underset{\sim}{p}'$. "Glancing blow" collisions may under certain conditions become the major contribution to the differential reactive cross section.

39. R. B. Bernstein and R. D. Levine, J. Chem. Phys. <u>49</u>, 3872 (1968).

40. T. T. Warnock and R. B. Bernstein, J. Chem. Phys. <u>49</u>, 1878 (1968); <u>ibid</u>. <u>51</u>, 4682 (1969).

C2

41. This is a good example of one of the goals in developing this model: isolation of the kinematics from the chemistry. The kinematics alone predict an angular distribution which is nearly isotropic for large α . Thus any observed departure from an isotropic distribution must be explained in terms of potential surface characteristics.

42. For the case $\alpha = 1.001$, $d^2\sigma(\chi)/d^2\omega$ is some five orders of magnitude larger at $\chi = 0°$ than at 10°. Thus even with the single constraint $\alpha \to 1$, the SS limit is very nearly approached. This limit is closely related to Herschbach's[20] modified SS model in which the internal momentum of BC is taken into account. There it is also found that the distribution of AB recoil vectors is strongly peaked forward but with a finite angular width.

43. From Eq. (I.11) the cause of the zero in the differential cross section is seen to be closely related to a semiclassical rainbow. For elastic scattering a rainbow is found when $\frac{d\chi}{db} = 0$, causing an infinity in the classical cross section. Here, $d\chi/d\theta = \infty$ causing a zero in the cross section.

44. A. M. Rulis and R. B. Bernstein, to be published.

45. G. H. Kwei, J. A. Norris, and D. R. Herschbach, J. Chem. Phys. 52, 1317 (1970). This paper reports results for $K + CH_3I$; however the authors have also obtained results for $Rb + CH_3I$. Their results are quoted in Ref. 21.

46. One might also examine the trends in the angular distributions for the reactions of CH_3I with various alkalis. For these systems the most probable α's lie in the range 10-20, so that the model predicts

very similar angular distributions for the entire series. The small mass effect calculated (assuming identical values for the most probable E'/E) produces an angular distribution slightly more concentrated in the backward direction as the alkali mass is reduced. This is contrary to the experimental findings of D. D. Parrish and R. R. Herm, J. Chem. Phys. 54, 2518 (1971) who report a LiI distribution broader than for the other alkali iodides.

47. R. Grice and P. B. Empedocles, J. Chem. Phys. 48, 5352 (1968).

48. D. D. Parrish and R. R. Herm, J. Chem. Phys. 51, 5467 (1969).

49. (a) J. H. Birely, R. R. Herm, K. R. Wilson, and D. R. Herschbach, J. Chem. Phys. 47, 993 (1967); see also (b) J. H. Birely and D. R. Herschbach, ibid. 44, 1690 (1966).

50. T. T. Warnock, R. B. Bernstein, and A. E. Grosser, J. Chem. Phys. 46, 1685 (1967).

51. As mentioned earlier, a negative impulse may be thought of as representing attraction between reactants in the entrance channel. This is in accord with current interpretations of this reaction mechanism based on the "electron-jump" model.

52. K. T. Gillen, A. M. Rulis, and R. B. Bernstein, J. Chem. Phys. 54, 2831 (1971).

53. However, the average deviation between the contour maps back-calculated from the model and the experimental maps was fairly large (ca. ± 20%). Thus, as expected, such detailed flux contour maps contain more than simple kinematic and conservation-governed information.

54. K. T. Gillen, C. Riley, and R. B. Bernstein, J. Chem. Phys. 50, 4019 (1969).

55. L. R. Martin and J. L. Kinsey, J. Chem. Phys. 46, 4834 (1967); the backscattering of KBr from K + TBr has recently been confirmed by L. R. Martin who has performed these experiments on a different machine (private communication).

56. A. C. Roach, Chem. Phys. Lett. 6, 389 (1970) has rationalized the isotope effect for this reaction using the DIPR model.

57. For K + HBr, $\Delta D_o = 4.75$ kcal/mole and for the values chosen for E_{tr}, E_{rot} and E'_{tr}, E'_{rot} (max) = 6.2 kcal/mole.

58. E. F. Greene, A. L. Moursund, and J. Ross, Adv. Chem. Phys. 10, 135 (1966).

59. R. Grice, J. E. Mosch, S. A. Safron, and J. P. Toennies, J. Chem. Phys. 53, 3376 (1970).

60. C. Maltz and D. R. Herschbach, Discussions Faraday Soc. 44, 176 (1967).

61. J. H. Birely, E. A. Entemann, R. R. Herm, and K. R. Wilson, J. Chem. Phys. 51, 5461 (1969).

62. G. Herzberg, Spectra of Diatomic Molecules (D. Van Nostrand Co., N. Y. 1950).

63. Whether above or below depends on which direction b increases. We define a positive b to mean that A has an algebraically smaller x-value than the c.m. of BC.

64. R. B. Bernstein, Adv. Chem. Phys. 10, 75 (1966).

65. The rainbow singularities are removed when the differential cross section is averaged over θ and ϕ.

66. Y. T. Lee, R. J. Gordon, and D. R. Herschbach, J. Chem. Phys. 54, 2410 (1971).

67. This symmetry is not necessary because the model distinguishes between the Cs atoms as B and C. A weighting function can easily be imagined, e.g. $(\theta/90)e^{-(\theta/90)}$, which destroys this symmetry and provides distinct results for positive and negative impulses.

LEGENDS FOR FIGURES

Fig. 1. (a) Momentum diagram illustrating Eq. (6) for the impulse $\underset{\sim}{I}$. For the case shown ($\alpha < 1$), $\chi < \pi/2$ (forward scattering). (b) Coordinate diagram, with origin at the center of mass of BC. The initial relative velocity $\underset{\sim}{g}$ defines the Z direction. R specifies the "reaction radius" and b is the impact parameter. A and the c.m. of BC lie in the XZ-plane.

Fig. 2. Weighting functions R_θ, $\langle T_\theta \rangle$ and $\langle T_\theta P_b \rangle$. The averages are over b, ϕ. The functions are arbitrarily scaled to unity at $\theta = 0$.

Fig. 3. Plots of $d^2\sigma_R(\chi)/d^2\omega$ for various values of α and for R = 2. The weighting function is $(1 \pm \cos\theta)^n$ where each curve is labelled with the choice of sign and the value of n.

Fig. 4. Plot of configuration angle θ versus scattering angle χ for $\alpha = 0.8$. Vector diagrams, similar to Fig. 1, have been drawn for small and large values of χ. It can be seen that only configurations with $\theta < 90°$ are possible.

Fig. 5. Plot of $d^2\sigma_R(\chi)/d^2\omega$ for Rb + CH_3I. The weighting parameter is n = 1.

Fig. 6. Plot of $d^2\sigma_R(\chi)/d^2\omega$ for the reactions K + Cl_2, Br_2, and I_2. Model parameters: negative impulse, α based on Q = 0, and weighting parameter n = 1.

Fig. 7. Plot of δ_{rot} defined in Eq. (21), versus scattering angle χ for the systems Li, K, Cs + Br_2. Model parameters are given in Table 3.

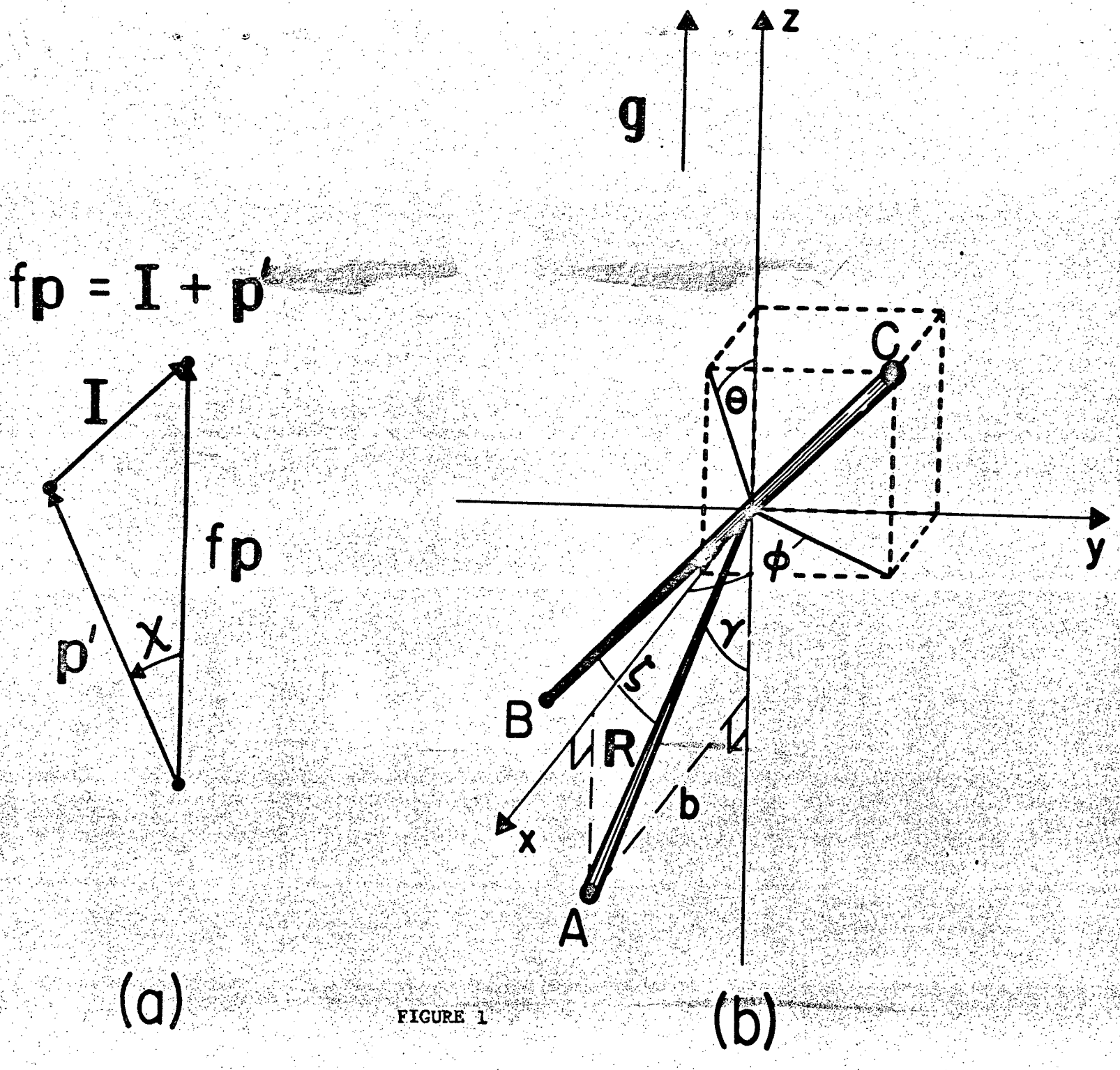

FIGURE 1

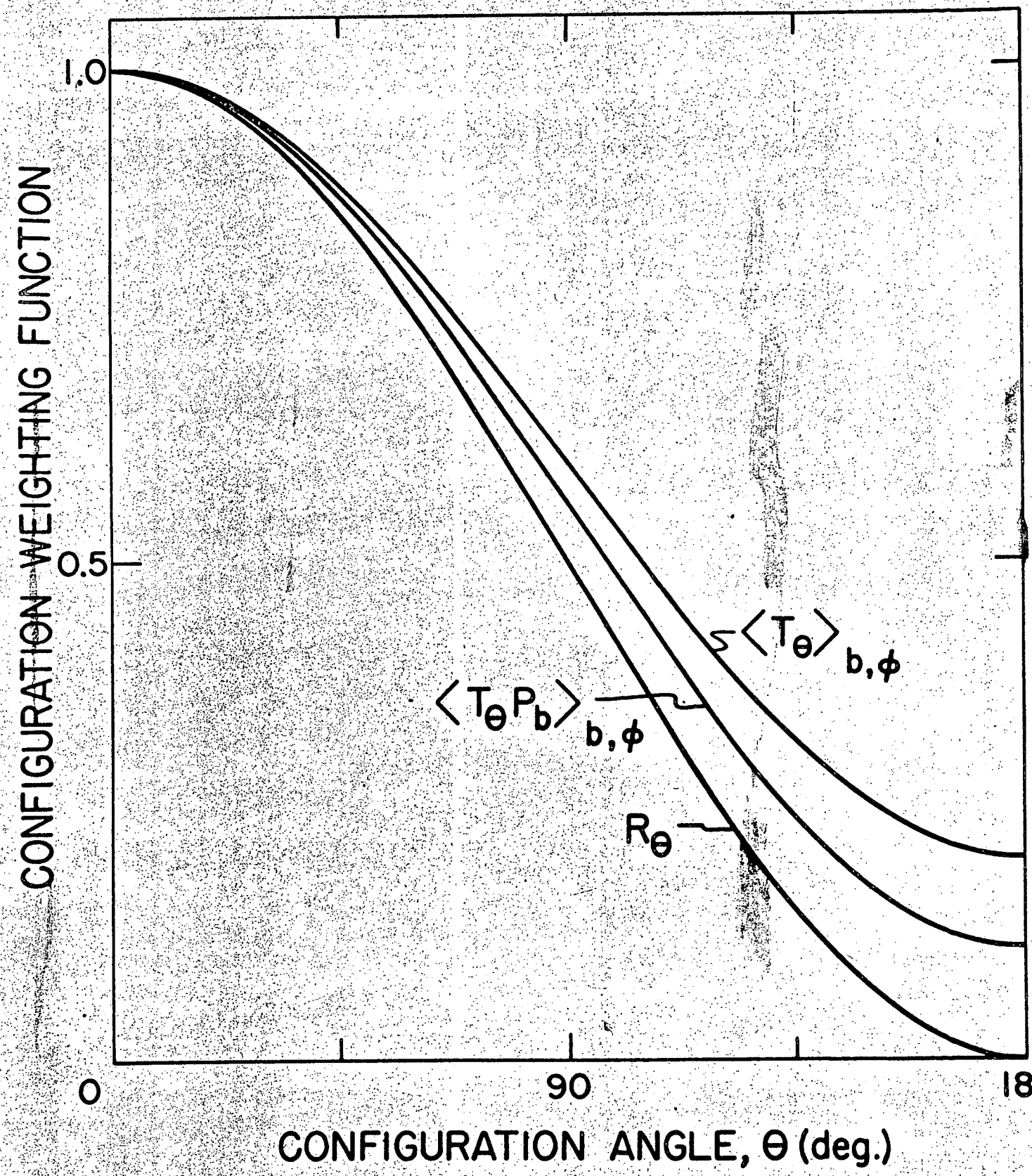
1.0
0.5
0
90
180
CONFIGURATION WEIGHTING FUNCTION
CONFIGURATION ANGLE, Θ (deg.)
$\langle T_\theta \rangle_{b,\phi}$
$\langle T_\theta P_b \rangle_{b,\phi}$
R_θ

FIGURE 2

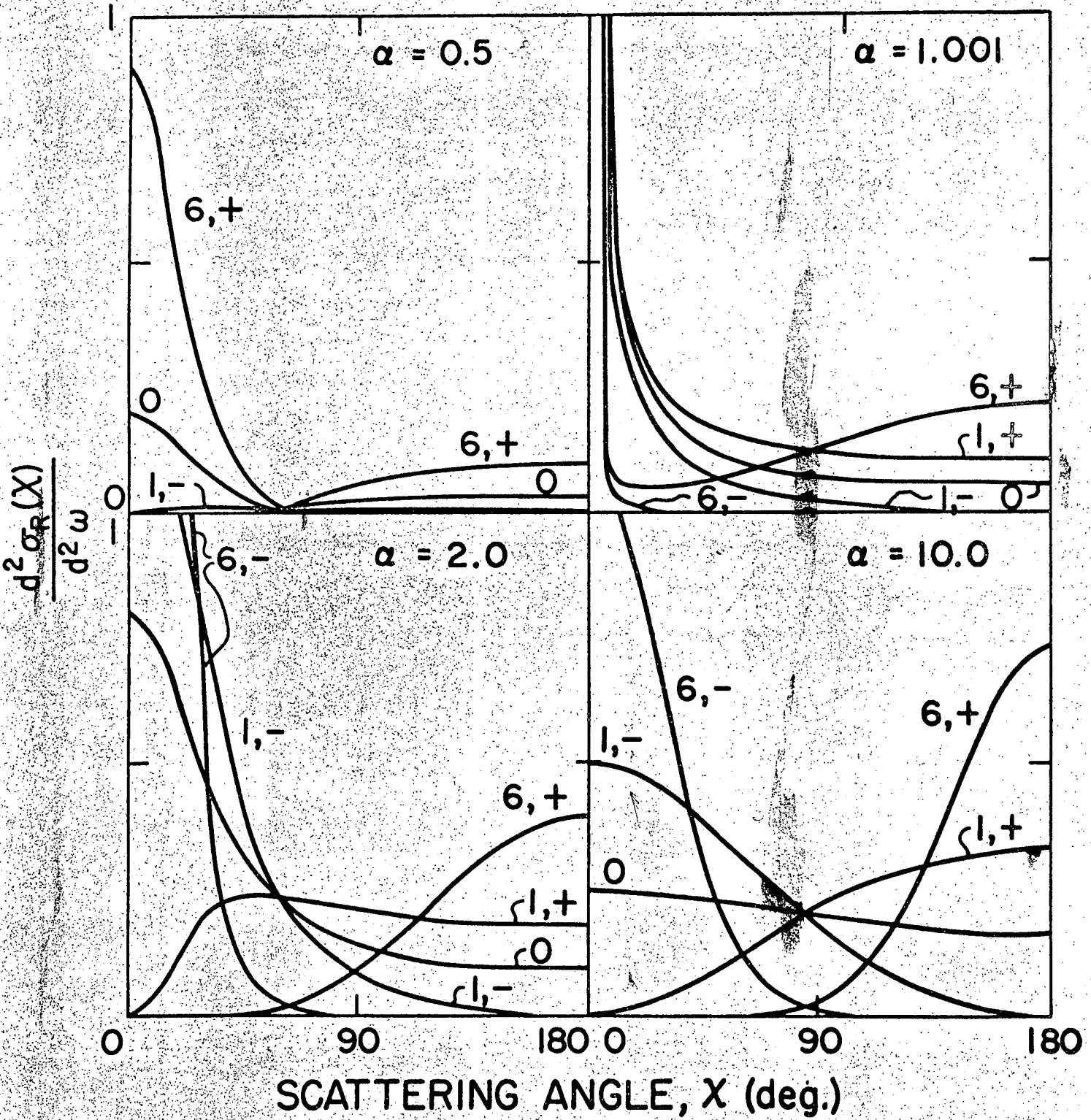
α = 0.5
α = 1.001
α = 2.0
α = 10.0
6,+
0
1,−
6,−
1,+
$\frac{d^2\sigma_R(\chi)}{d^2\omega}$
1
0
0
90
180
SCATTERING ANGLE, χ (deg.)

FIGURE 3

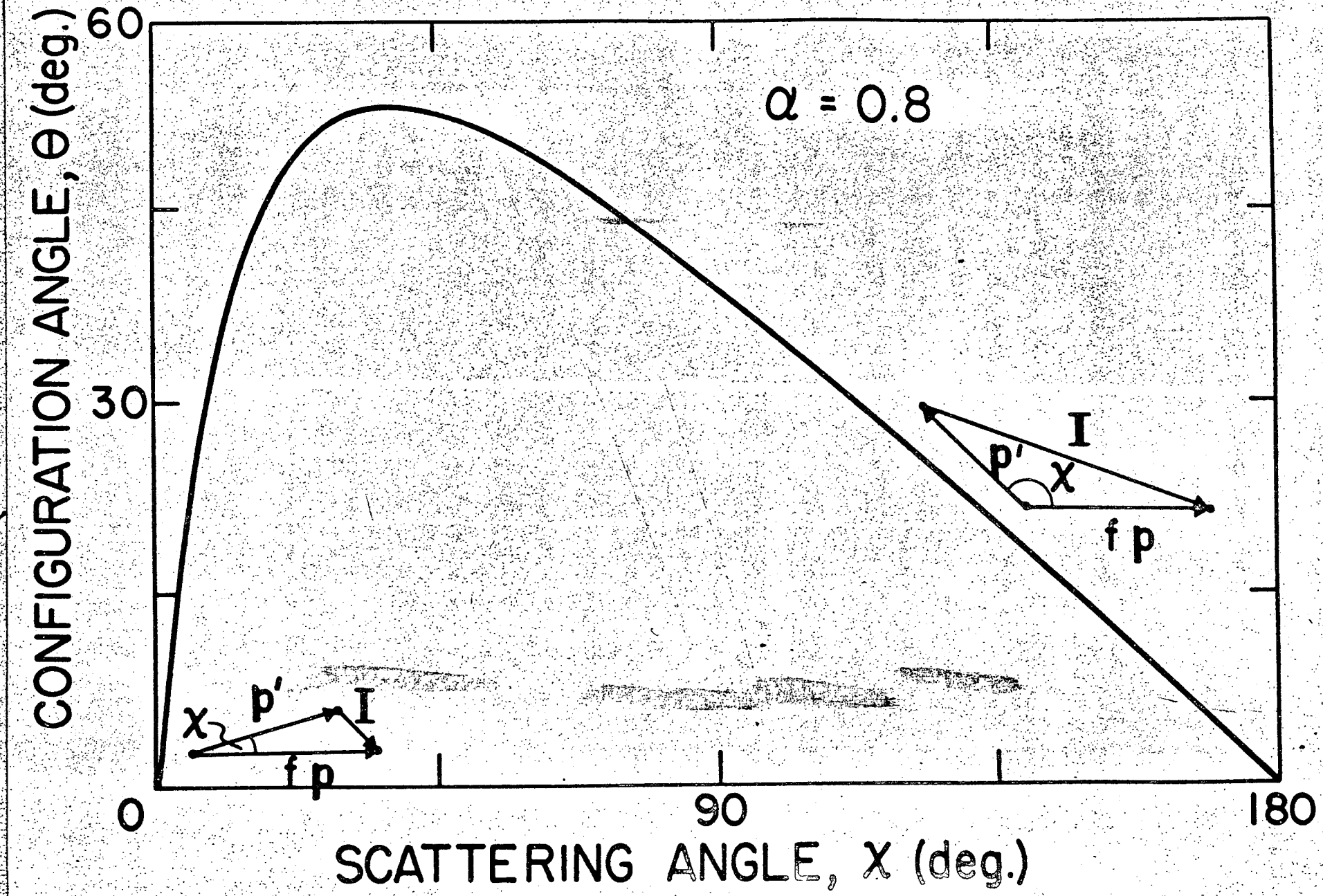
α = 0.8
CONFIGURATION ANGLE, Θ (deg.)
60
30
0
90
180
SCATTERING ANGLE, X (deg.)
I
p'
χ
f p
χ
p'
I
f p

FIGURE 4

FIGURE 5

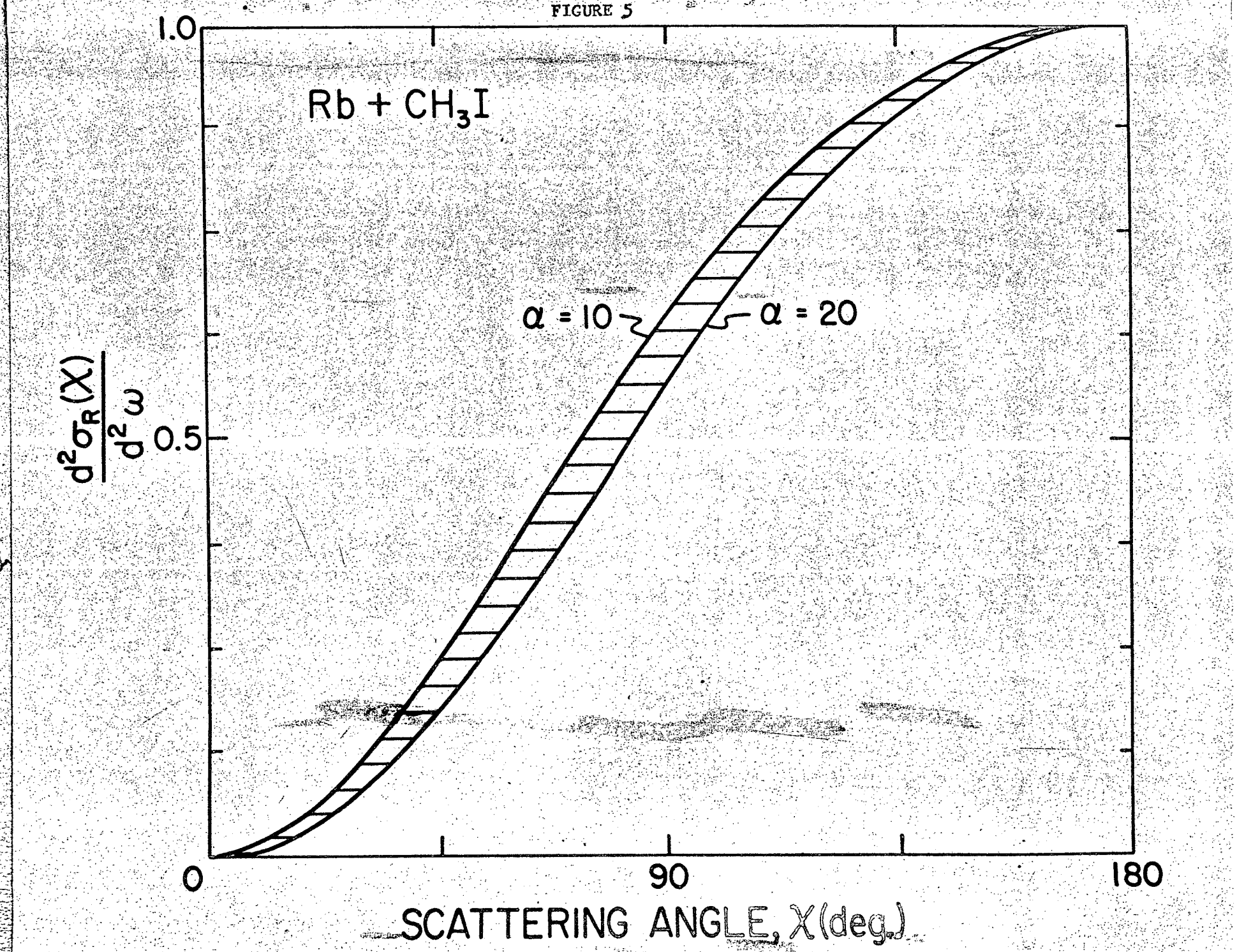

FIGURE 6

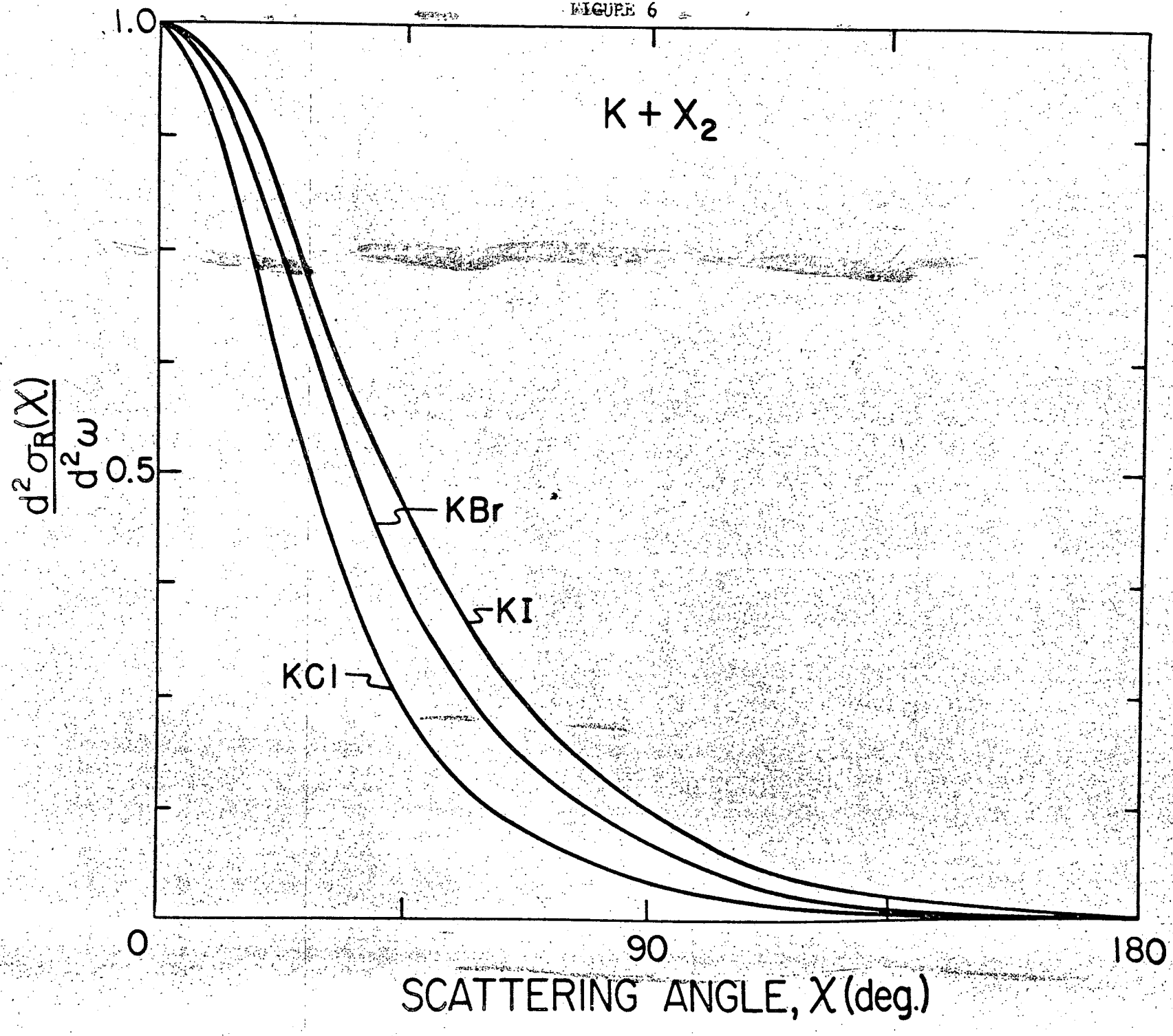
1.0
0.5
0
90
180
K + X2
KBr
KI
KCl
$\frac{d^2\sigma_R(\chi)}{d^2\omega}$
SCATTERING ANGLE, χ (deg.)

FIGURE 7